

Determinants of RING-E2 Fidelity for Hrd1p, a Membrane-anchored Ubiquitin Ligase*[§]

Received for publication, August 25, 2006, and in revised form, October 10, 2006. Published, JBC Papers in Press, October 11, 2006, DOI 10.1074/jbc.M608174200

Omar A. Bazirgan¹, Renee M. Garza¹, and Randolph Y. Hampton²

From the Section of Cell and Developmental Biology, Division of Biological Sciences, University of California, San Diego, La Jolla, California 92093

A critical aspect of E3 ubiquitin ligase function is the selection of a particular E2 ubiquitin-conjugating enzyme to accomplish ubiquitination of a substrate. We examined the requirements for correct E2-E3 specificity in the RING-H2 ubiquitin ligase Hrd1p, an ER-localized protein known to use primarily Ubc7p for its function. Versions of Hrd1p containing the RING motif from homologous E3s were unable to carry out Hrd1p function, revealing a requirement for the specific Hrd1p RING motif *in vivo*. An *in vitro* assay revealed that these RING motifs were sufficient to function as ubiquitin ligases, but that they did not display the E2 specificity predicted from *in vivo* results. We further refined the *in vitro* assay of Hrd1p function by demanding not only ubiquitin ligase activity, but also specific activity that recapitulated both the E2 specificity and RING selectivity observed *in vivo*. Doing so revealed that correct E2 engagement by Hrd1p required the presence of portions of the Hrd1p soluble cytoplasmic domain outside the RING motif, the placement of the Hrd1p ubiquitin ligase in the ER membrane, and presentation of Ubc7p in the cytosolic context. We confirmed that these conditions supported the ubiquitination of Hrd1p itself, and the transfer of ubiquitin to the prototype substrate Hmg2p-GFP, validating Hrd1p self-ubiquitination as a viable assay of ligase function.

Ubiquitin is a covalent protein tag that alters the stability or behavior of a growing list of proteins (1–4). Covalent attachment of ubiquitin to target proteins occurs by a cascade of enzymes, beginning with a ubiquitin-activating enzyme (E1)³

hydrolyzing ATP to form a thioester-linked ubiquitin-bound intermediate. The E1 next passes its ubiquitin to a ubiquitin-conjugating enzyme (E2), again as a thioester-linked intermediate. Finally, ubiquitination of the target protein is brokered by a ubiquitin ligase (E3) that facilitates transfer of ubiquitin from the E2 to a lysine on the target protein (or a previously added ubiquitin) to form an isopeptide bond. *In vivo* the ubiquitin ligase activity of a given E3 is not universally supported by all E2s (5, 6). A typical E3 will function with only one or two of many E2s *in vivo* (7–11). Thus, the compatibility between E3 and E2 is a critical aspect of this enzyme cascade.

Many E3s share a zinc-binding sequence called the RING motif (12). This characteristic sequence, along with several variants (13, 14), is found in a large number of known or putative E3s, where it is required for ubiquitin ligase activity both *in vivo* and *in vitro* (8, 9, 11, 15–17). Unlike the HECT domain ligases, the RING ligases and their variants do not form a covalent adduct with ubiquitin during catalysis (18, 19). Despite the prevalence of RING motifs among the growing number of ubiquitin ligases, and their necessity for ligase function in these proteins, the role of the RING motif in promoting E2 specificity and ubiquitin transfer is not fully understood. Structural analyses suggest that residues in the RING motif make contact with E2s, but so too do some residues outside the RING motif (20–23). It is not clear whether the RING motif alone is sufficient to specifically engage an E2 and stimulate ubiquitination activity, or whether other *in cis* determinants outside the RING motif contribute to E2 selectivity. We have addressed these questions for the case of the ubiquitin ligase Hrd1p.

A significant component of protein degradation in eukaryotes occurs at the surface of the ER and is generally referred to as ERAD, for ER-associated degradation. ERAD is responsible for degradation of a variety of integral membrane and luminal proteins in the ER (24). The Hrd1p ubiquitin ligase in *Saccharomyces cerevisiae* is one of several E3s that mediate ERAD (9, 10, 25), with homologs in all eukaryotes (26, 27). Hrd1p is responsible for the degradation of the yeast HMG-CoA reductase isozyme Hmg2p (28), and a variety of misfolded ER proteins (29–31). Hrd1p consists of an N-terminal multi-spanning membrane anchor and a cytoplasmic C-terminal region bearing a RING-H2 motif. The cytoplasmic portion is required for Hrd1p-dependent ERAD *in vivo* (16) and functions

extension; GFP, green fluorescent protein; AEBF, 4-(2-aminoethyl)benzenesulfonyl fluoride; PMSF, phenylmethylsulfonyl fluoride; TPCK, 1-chloro-3-tosylamido-4-phenyl-2-butanone; MOPS, 3-(*N*-morpholino)propanesulfonic acid; DTT, dithiothreitol; WT, wild type; GST, glutathione S-transferase.

* This work was supported by Grant GM51996-06 from the NIDDK, National Institutes of Health (to R. Y. H.) and the American Heart Association (Established Investigator Award, to R. Y. H.). The costs of publication of this article were defrayed in part by the payment of page charges. This article must therefore be hereby marked "advertisement" in accordance with 18 U.S.C. Section 1734 solely to indicate this fact.

R. Y. H. wishes to dedicate this work to the memory of Dr. Robert MacFarlane. He was a non-Euclidian (that is, without parallel) intellectual and spiritual guide who will be missed by many.

[§] The on-line version of this article (available at <http://www.jbc.org>) contains supplemental Tables S1 and S2.

¹ Supported in part by an National Institutes of Health Training Grant GM07240.

² To whom correspondence should be addressed: Section of Cell and Developmental Biology, Division of Biological Sciences, University of California, San Diego, 9500 Gilman Drive, La Jolla, CA, 92093-0347. Tel.: 858-822-0511; Fax: 858-534-0555; E-mail: rhampton@biomail.ucsd.edu.

³ The abbreviations used are: E1, ubiquitin-activating enzyme; E2, ubiquitin-conjugating enzyme; E3, ubiquitin ligase; ERAD, endoplasmic reticulum-associated degradation; CBD, chitin-binding domain; Hmg-CoA, 3-hydroxy-3-methylglutaryl CoA; HA, hemagglutinin; SOEing, strand overlap

Determinants of RING-E2 Fidelity for Hrd1p

autonomously as a ubiquitin ligase *in vitro* (9). Hrd1p is complexed with the ER integral membrane protein Hrd3p. One function of Hrd3p is to promote Hrd1p stability. In the absence of Hrd3p, Hrd1p undergoes rapid degradation mediated by the Hrd1p RING-H2 motif resulting in Hrd1p levels too low to sustain ERAD (16). If Hrd1p levels are elevated in the absence of Hrd3p, ERAD will proceed, indicating that Hrd1p is a key protein of HRD pathway ubiquitination (16).

The cytoplasmic C-terminal RING-H2 domain of Hrd1p is exposed to numerous ubiquitin E2s; yet, Hrd1p only employs Ubc7p, and to a much lesser extent Ubc1p, in the execution of its function (9). This same E2 specificity is observed for Hrd1p self-ubiquitination in the absence of Hrd3p (16). However, the Hrd1p RING domain will function *in vitro* with E2s that are not used *in vivo* (9), leading us to wonder which features of Hrd1p contribute to its high selectivity for Ubc7p *in vivo*. In particular, we were interested in developing biochemical approaches for studying Hrd1p action that would faithfully recapitulate this selectivity in biochemically tractable conditions. We have determined that *cis*-acting portions of Hrd1p, the membrane anchoring protein Cue1p, and the placement of Hrd1p in the ER membrane bilayer are all critical to reconstituting *in vitro* the function of Ubc7p with Hrd1p.

EXPERIMENTAL PROCEDURES

Recombinant DNA—Detailed plasmid information is available in supplemental data. PCR primer information will be provided upon request. All DNA segments synthesized by PCR were verified by sequencing. The production of coding regions was described for Hrd1p-3HA and C399S Hrd1p-3HA (16), as well as Ubc7p-2HA (32). gp78, hsHrd1, and Praja1 RING motifs were amplified by PCR from published template plasmids (15, 33), and joined to Hrd1p sequences by a PCR SOEing method to precisely replace the native Hrd1p RING motif (34, 35), and subcloned into plasmids containing Hrd1p-3HA to yield gp78, hsHrd1, or Praja1 RING chimera in otherwise full-length Hrd1p-3HA. These were then subcloned into yeast expression plasmids with either the native *HRD1* promoter or the strong *TDH3* promoter. Hrd1p- Δ pro was made using PCR SOEing to join the sequences of Hrd1p on either side of the proline-flanked deletion (see Fig. 1), and subcloned into appropriate Hrd1p-3HA plasmids. C399A-Hrd1p was made by PCR SOEing, and was found to be as potent a RING mutant as C399S-Hrd1p (data not shown).

All GST fusions were expressed from the pET42b(+) bacterial expression plasmid (Novagen). The isolated RING motifs were amplified by PCR from plasmids above and subcloned into pET42b(+). pRH1466, the plasmid expressing GST-R-C, was previously described (9). GST-N-R and GST-N-R-C were made by PCR of the appropriate sequence from Hrd1p plasmid and subcloning into pRH1466. GST-N-c399s-C and GST-N-gp78-C were made by PCR of sequence encoding the mutant C399S-Hrd1p or chimeric gp78-RING-Hrd1p. The c399 refers to the last cysteine of the Hrd1p RING that normally occupies position 399 of full-length Hrd1p.

The Ubc7p or Ubc7p-2HA coding region was amplified by PCR and subcloned into pTYB2 (New England Biolabs) to produce the Ubc7p-Chitin Binding Domain/Intein fusion vector

pRH1946. Δ tmCue1p, which lacks amino acids 2–22 of Cue1p (and thus the included transmembrane span) was amplified by PCR from pTX129 (36) and cloned into a pET bacterial expression vector. Then, the ribosomal binding site and Δ tmCue1p were amplified by PCR and cloned behind Ubc7p-CBD/Intein in pRH1946 to produce pRH2061, with a polycistronic message encoding both Ubc7p-CBD/Intein and Δ tmCue1p proteins in one inducible operon. His₆-tagged mouse UBA1 (E1) and HUBC4 were purified from bacterial lysates as described previously (9, 37, 38).

Strains and Media—Yeast were cultured at 30 °C as described (28, 39), in minimal media with 2% glucose and amino acid supplements. Detailed strain information is presented in supplemental data. All yeast strains were derived from the same genetic background used in our previous work (28, 39). Strains for evaluating the *in vivo* degradation of Hmg2p-GFP were derived from the previously described RHY853 (16), expressing Hmg2-GFP and the independently expressed catalytic domain of Hmg2p as its sole source of HMG-CoA reductase. *HRD1* was replaced in RHY853 with the G418-resistance marker kanMX (40) to produce RHY2814. The various HA epitope-tagged Hrd1p chimeric RING plasmids or controls were integrated into this *hrd1* Δ strain at the *TRP1* locus. To evaluate Hrd1p degradation, *HRD3* was deleted in RHY2814 with the selectable *LEU2* marker to produce RHY3005. Into this *hrd1* Δ *hrd3* Δ strain, the various Hrd1p RING replaced plasmids or controls were also integrated at the *TRP1* locus. To evaluate Ubc7p dependence of Hrd1p degradation, *UBC7* was deleted in RHY3005 with the nourseothricin-(ClonNat) resistance marker natMX (41) to produce RHY3559, into which Hrd1p RING replaced plasmids or controls were integrated at the *TRP1* locus.

Strains used to produce microsomal membranes for the *in vitro* assay were *pep4* Δ *ubc7* Δ *hrd1* Δ , and expressed Hmg2p-GFP. The full-length Hrd1p-3HA chimeras tested in microsomes were expressed in these strains from the strong *TDH3* promoter by integration of the appropriate plasmid at the *TRP1* locus. *cue1* Δ nulls were generated from these strains by deletion of *CUE1* with the nourseothricin (ClonNat) resistance marker natMX (41). Strains for the production of cytosol were also *pep4* Δ *hrd1* Δ *ubc7* Δ and included either empty vector or Ubc7p-2HA expressed from the *TDH3* promoter.

Flow Cytometry—Log phase cultures ($A_{600} < 0.5$) grown in minimal medium at 30 °C were transferred to flow cytometer sample tubes and measured with a Becton Dickinson FACScalibur instrument. Flow microfluorimetric data were analyzed and histograms were generated using CellQuest flow cytometry software. In all cases, histograms represented 20,000 individual cells.

Cycloheximide Chase Degradation Assay—This assay was performed as described (39). Briefly, log phase cultures of cells expressing HA epitope-tagged Hrd1p or RING variants were treated with 50 μ g/ml cycloheximide to arrest protein synthesis. At indicated times, 1 OD of log phase cells were harvested, lysed, and 0.1 OD equivalents were resolved by SDS-PAGE and immunoblotted for epitope-tagged protein.

Protein Purification—All recombinant proteins were expressed in Rosetta(DE3) *Escherichia coli* (Novagen) grown in

LB with appropriate antibiotics. 0.6 OD/ml cultures were induced with 0.5 mM isopropyl-1-thio- β -D-galactopyranoside for 12–16 h at 15 °C. Bacterial pellets were harvested, washed in normal saline (0.9 M NaCl), and frozen at –80 °C. Pellets were thawed and resuspended in extraction buffers as described below, and lysed using a Branson Sonifier 450 (VWR) with six rounds of 30 s sonication/30 s ice incubation. After affinity column purification, elution, and concentration, proteins were dialyzed into buffer HDB containing 10% glycerol. Single use aliquots were flash-frozen with liquid nitrogen and stored at –80 °C. Recombinant protein concentrations were determined by Coomassie staining of SDS-PAGE resolved samples and comparison to bovine serum albumin.

His Tag Purification of E1 and HUBC4—Bacterial pellets from 2-liter cultures expressing His₆ mouse UBA1 or HUBC4 were resuspended in 40 ml of His-Extraction Buffer (50 mM sodium phosphate pH 7.4, 300 mM NaCl, 0.5% Nonidet P-40, 5% glycerol) with protease inhibitors (13 μ M AEBSE, 3.6 μ M TPCK, 2.6 μ M leupeptin, 1.8 μ M pepstatin, 0.56 mM 6-amino-hexanoic acid, 0.56 mM benzamidine, and 2.5 mM 2-mercaptoethanol), sonicated as above, and centrifuged at 12,000 \times g for 20 min in an SS34 rotor. The supernatant was transferred to a new tube with 0.5 ml of Talon Cell-Thru resin (BD Biosciences) equilibrated in His-Extraction Buffer, and gently nutated for 20 min at room temperature. The resin was centrifuged (3000 \times g) and washed with 10 ml of His-Extraction Buffer and protease inhibitors above for 10 min at room temperature two times. The washed resin was then transferred to a 1-cm diameter column and washed with 30 ml of His-Wash Buffer (50 mM sodium phosphate, pH 7.8, 300 mM NaCl, 5 mM imidazole, 5% glycerol, 10 mM 2-mercaptoethanol). His-tagged E1 was eluted from the resin with 3 ml of His-Wash Buffer + 150 mM imidazole, and was collected in 500- μ l fractions and analyzed by Bradford assay with bovine serum albumin standard. Fractions with more than 0.1 mg/ml protein were pooled and concentrated with Amicon Ultra-15 5,000 MWCO filters (Millipore). Concentrated protein was dialyzed over 24 h with 3 \times 1 liter HDBG (25 mM HEPES, 0.7 mM sodium phosphate, 137 mM NaCl, 5 mM KCl, pH 7.4, 10% glycerol) in a 3-ml 10,000 MWCO Slide-A-Lyser cassette (Pierce).

GST Protein Purification—Each bacterial pellet from 1 liter of culture expressing a GST protein was resuspended in 25 ml of buffer HDB (25 mM HEPES, 0.7 mM sodium phosphate, 137 mM NaCl, 5 mM KCl, pH 7.4) + protease inhibitors (7.5 mM EDTA, 1.5 mM PMSF, 10 μ M leupeptin, 7 μ M pepstatin, 28 μ M TPCK, 130 μ M AEBSE, 2.5 mM 6-aminohexanoic acid, 2.5 mM benzamidine, and 7.5 mM DTT), and sonicated as above. To this was added 6 ml of 2.5 M NaCl, 600 μ l 1 M sodium phosphate, pH 7.4, and 1.2 ml of 25% Triton X-100. This was nutated 20 min at 4 °C, and centrifuged for 1 h at 40,000 \times g in SS34 rotor. Buffer HDBW (HDB + 20 mM sodium phosphate, pH 7.4, 10 mM 2-mercaptoethanol, 1% Triton X-100.) was added to the supernatant to a final volume of 50 ml along with 1 ml of glutathione-Sepharose-4B resin (Amersham Biosciences) and nutated for 1 h at 4 °C. The resin was transferred to a 1-cm diameter column and washed with 10 ml of each of the following buffers: HDBW with 1.25 mM PMSF and 5 mM EDTA; HDBW with 1.25 mM PMSF, 5 mM EDTA, and 0.5 M NaCl; HDBW with 0.5%

deoxycholate; HDBW with 0.5 M NaCl; and Final Wash (40 mM Tris, pH 8.0, 50 mM NaCl, 10 mM 2-mercaptoethanol). Protein was eluted in 1-ml fractions of Elution Buffer (20 mM Tris, pH 8, 10 mM 2-mercaptoethanol, 20 mM reduced glutathione) incubated with column resin for 10 min before recovery. Fractions were analyzed by Bradford assay with bovine serum albumin standard. Fractions with more than 0.1 mg/ml protein were pooled and concentrated with Amicon Ultra-15 5,000 MWCO filters (Millipore). Concentrated protein was dialyzed for 24 h with 3 \times 1 liter HDBG (25 mM HEPES, 0.7 mM sodium phosphate, 137 mM NaCl, 5 mM KCl, pH 7.4, 10% glycerol) in a 0.5 ml 3,000 MWCO Slide-A-Lyser cassette (Pierce).

Intein/Chitin Binding Domain Fusion Purification—Each bacterial pellet from 1 liter of culture expressing an Intein/CBD fusion was resuspended in 25 ml of Intein Lysis Buffer (ILB: 50 mM Tris, pH 8.0, 500 mM NaCl, 1 mM EDTA, 0.1% Triton X-100) with protease inhibitors (260 μ M AEBSE, 105 μ M leupeptin, 73 μ M pepstatin, 142 μ M TPCK), and sonicated as above. Lysate was centrifuged at 20,000 \times g for 30 min in an SS34 rotor. Supernatant was filtered through 0.45- μ m and 0.2- μ m filters, and added to 15 ml of chitin beads (New England Biolabs) equilibrated in ILB, and nutated for 90 min at 4 °C. The adsorbed resin was placed in a 2.5-cm column and washed with 350–400 mls of ILB. Next, the resin was nutated in 10 ml of ILB + 50 mM DTT for 20 h at 4 °C to promote intein cleavage, and chitin beads were washed with ILB to collect intein-cleaved proteins. 40 ml of fluid were collected and concentrated using Amicon Ultra-15 5,000 MWCO filters (Millipore). Concentrated protein was dialyzed against 3 \times 1 liter HDBG (25 mM HEPES, 0.7 mM sodium phosphate, 137 mM NaCl, 5 mM KCl, pH 7.4, 10% glycerol) for 24 h in a 0.5 ml 3,000 MWCO Slide-A-Lyser cassette (Pierce). Proteins were ultracentrifuged at 100,000 \times g to remove any aggregates, and supernatant was aliquoted as above.

In Vitro Ubiquitination—Ubiquitin was resuspended from lyophilized powder in Ubiquitin Storage Buffer (50 mM Tris, pH 7.5, 50 mM NaCl, 10% glycerol) and frozen. Reactions were performed in 1 \times ubiquitination buffer (50 mM Tris, pH 7.5, 2.5 mM MgCl₂, 0.5 mM DTT) with 3 mM ATP, 80 μ g/ml ubiquitin, 6 μ g/ml E1, 20 μ g/ml E2, in a total volume of 15 μ l. Reactions mixtures were prepared on ice, then incubated at 30 °C for 2 h, and stopped with an equal volume of 2 \times sample buffer (4% SDS (w/v), 8 M urea, 75 mM MOPS, pH 6.8, 200 mM DTT, 0.2 mg/ml bromphenol blue) and analyzed by SDS-PAGE and anti-ubiquitin immunoblotting.

Microsome Preparation and Ubiquitination—20 A₆₀₀ units of log phase cells grown in minimal media were harvested and resuspended in 400 μ l of ice-cold Membrane Fractionation Buffer (MFB: 20 mM Tris, pH 7.5, 0.1 M NaCl, 0.3 M sorbitol) with protease inhibitors (260 μ M AEBSE, 105 μ M leupeptin, 73 μ M pepstatin, 142 μ M TPCK). Glass beads were added to just below the liquid level. Lysis was performed at 4 °C with six cycles of 1min vortexing (max speed) and 1 min incubation on ice. Lysate was harvested by removing supernatant from beads, and washing beads twice with 400 μ l of MFB, pooling the washes and lysate. The resulting pooled lysate was cleared by repeated 10-s microcentrifuge pulses to remove unlysed cells and large debris. The cleared supernatant contains microsome

Determinants of RING-E2 Fidelity for Hrd1p

membranes, which were harvested by centrifugation at $21,000 \times g$ for 30 min. Microsome pellets were resuspended in 60 μ l of Ubiquitination Buffer, and the yield from 5 OD of cells (15 μ l) was added to each reaction. Reactions were performed in Ubiquitination Buffer with 6 μ g/ml E1, 40 μ g/ml E2 (except as noted in E2 dilution experiments), 160 μ g/ml ubiquitin, and 3 mM ATP in 60- μ l reactions. Reaction mixes were prepared on ice, then incubated at 30 °C for 2 h. Reactions were stopped with 200 μ l of SUME (1%w/v SDS, 8 M urea, 10 mM MOPS, pH 6.8, 10 mM EDTA) with protease inhibitors above and 5 mM *N*-ethylmaleimide, followed by addition of 600 μ l of IP buffer (15 mM sodium phosphate, 150 mM NaCl, 10 mM EDTA, 2% Triton X-100, 0.1% SDS, 0.5% deoxycholate), immunoprecipitation of Hrd1p as described (9), and immunoblotting the SDS-PAGE resolved immunoprecipitate for ubiquitin with anti-ubiquitin antibodies (Zymed Laboratories, South San Francisco, CA) or for Hrd1p with anti-HA ascites fluid (Jackson ImmunoResearch).

Microsome Ubiquitination Assay with Cytosol—Cytosol and microsomes were prepared as previously described (42). Briefly, microsomes were prepared as above and resuspended in 60 μ l of B88 buffer (20 mM HEPES pH 6.8, 250 mM sorbitol 150 mM KOAc, 5 mM MgOAc, 1 mM DTT) with protease inhibitors (1 mM PMSF, 260 μ M AEBSEF, 100 μ M leupeptin, 76 μ M pepstatin A, 5 mM 6-aminohexanoic acid, 5 mM benzamidin, and 142 μ M TPCK). At the same time, cytosol from a Ubc7p overexpressing, *hrd1* Δ -null strain was prepared in the manner of Spang and Schekman (43). Control cytosol was prepared in parallel from an otherwise identical *ubc7* Δ -null strain. Briefly, 500 OD equivalents of cells were pelleted, rinsed once with water, once with B88 buffer, and resuspended in 500 ml of B88 buffer. The resulting suspension was poured into a liquid nitrogen-containing mortar, and the resulting fast-frozen pellet was ground with a pestle until a fine powder. The frozen powder was next transferred to a microcentrifuge tube, raised to 1 mM ATP with a 500 mM stock solution in water (pH 7.5), and allowed to thaw on ice. The thawed cytosol lysate was centrifuged at $3000 \times g$ for 5 min, to remove debris, and the resulting supernatant was removed and centrifuged at $20,000 \times g$ for 15 min. Finally, the resulting $20,000 \times g$ supernatant was removed and ultracentrifuged ($100,000 \times g$) for 1 h. The resulting supernatant was collected, and diluted to 25 mg/ml protein for use in the ubiquitination assay. The *in vitro* ubiquitination assay was initiated by addition of 20 μ l of microsomes (with Hrd1p and Hmg2p), 12 μ l of cytosol, and sufficient concentrated stock of ATP to yield 30 mM ATP, followed by incubation at 30 °C, typically for an hour. The assay was terminated by solubilization with 200 μ l of SUME with protease inhibitors above and 5 mM *N*-ethylmaleimide, followed by addition of 600 μ l of IP buffer, and subsequent immunoprecipitation of either Hrd1p or Hmg2p. Immunoprecipitated samples were SDS-PAGE resolved and immunoblotted for ubiquitin and for either Hrd1p or Hmg2p-GFP using anti-HA ascites fluid, or anti-GFP monoclonal antibodies as described (9).

RESULTS

Removal or mutation of the Hrd1p RING motif eliminates Hrd1p function (9, 16). To more fully understand the role of the

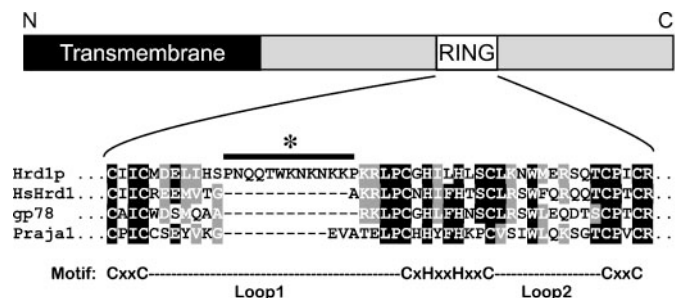


FIGURE 1. RING motifs used to replace the native RING in Hrd1p. Schematic depiction of Hrd1p, and sequence alignment of RING-H2 motifs used to replace Hrd1p RING sequence in otherwise full-length Hrd1p. Loop1 and Loop2 represent variable sequences in between conserved cysteine/histidine residues that define the RING motif. Asterisk indicates sequence of Hrd1p in Loop1 that was removed in the Hrd1p- Δ pro mutation.

Hrd1p RING in E2 selection we created versions of the *HRD1* coding region expressing Hrd1p with RING motifs from other ubiquitin ligases. We chose the RING sequences from gp78, hsHrd1/synoviolin, and Praja1 (Fig. 1). gp78 is a ubiquitin ligase involved in ERAD that engages a mammalian homolog of Ubc7p (Ube2G2) (17, 44, 45). hsHrd1 is another mammalian ligase implicated in ERAD (27, 33, 46, 47), and both gp78 and hsHrd1 are the nearest mammalian homologs to Hrd1p. Praja1 is a ligase with no known function in ERAD (48, 49), but like the others has been observed to form ubiquitin chains *in vitro* (15). To test these RING motifs *in vivo*, 3HA-tagged constructs of Hrd1p with replaced RING sequences or a wild-type Hrd1p RING control were expressed from the native promoter as single copy integrants in a *hrd1* Δ -null strain and tested for ability to degrade Hmg2p-GFP, which can be assayed both biochemically and by flow cytometry (9, 50, 51).

When Hmg2p-GFP is expressed in a *hrd1* Δ -null, its steady-state levels are high because it cannot be degraded (16). The increased fluorescence of *hrd1* Δ cells is revealed by a fluorescence histogram strongly shifted to the right (Fig. 2A, empty vector). Expression of wild-type *HRD1* restores degradation of Hmg2p-GFP, lowering steady-state Hmg2p-GFP levels, and shifting the fluorescence histogram to the left (Fig. 2A, WT). Expression of the inactivated C399S mutant of Hrd1p is unable to support Hmg2p-GFP degradation, as shown by overlap of the C399S strain's histogram with the *hrd1* Δ -null mutant (Fig. 2A, C399S). Using this assay we tested the activity of the RING-replaced Hrd1p variants. The chimeric Hrd1p constructs with RING motifs from gp78, hsHRD1 and Praja1 were all unable to function when expressed at native levels *in vivo*, as indicated by the overlapping of histograms with those of *hrd1* Δ -null or C399S strains (Fig. 2A), or the mean fluorescence of the cell populations (Fig. 2B). Overexpressing each chimeric Hrd1p from the strong *TDH3* promoter (about 30-fold higher expression by immunoblotting) caused slight but reproducible suppression of the ERAD defect (Fig. 2C), with gp78-RING-substituted Hrd1p having the most activity, about 1/8 that of authentic Hrd1p in lowering Hmg2p-GFP steady-state levels. As expected, native *HRD1* expressed at these levels caused further degradation of the reporter, because it is rate-limiting for degradation of Hmg2p (9, 16). In each experiment, all Hrd1p proteins were expressed at similar levels as discerned by immunoblotting (Fig. 2D and data not shown). Thus, even function-

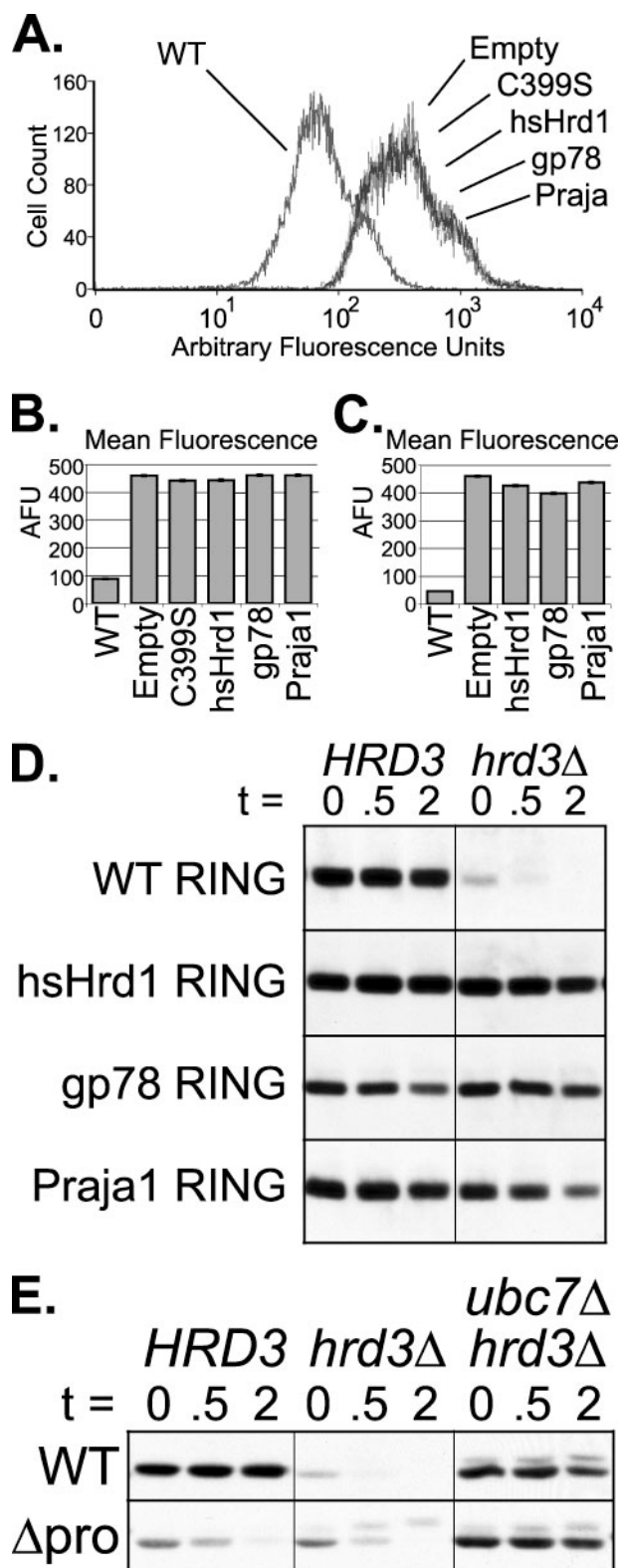


FIGURE 2. Hrd1p with replaced RINGs do not function. *A*, WT and the described RING-replaced versions of Hrd1p were expressed from the *HRD1* promoter in strains with a *hrd1Δ*-null allele and expressing Hmg2p-GFP. For each strain, fluorescence of 20,000 cells was measured by flow cytometry. Histograms were generated by plotting the number of cells (y-axis) having a given arbitrary fluorescence (x-axis). Degradation of Hmg2p-GFP was restored only by the WT RING version of Hrd1p, and none of the others tested. *B*, mean fluorescence from histograms in *A*. Error bars depict the S.E. *C*, overexpression of replaced-RING-Hrd1p does not support ERAD. WT and replaced-RING versions of Hrd1p were expressed from the strong

ally related RING-H2 motifs from mammalian ERAD ubiquitin ligases were not sufficient to restore normal Hrd1p-dependent ERAD *in vivo*.

RING E3s mediate transfer of ubiquitin from E2 to substrate. The lack of *in vivo* function in the chimeric Hrd1p proteins could either be due to an inability to engage the Ubc7p E2, or an inability to catalyze transfer of ubiquitin to the Hmg2p-GFP substrate. These two possibilities could be distinguished experimentally, because native Hrd1p undergoes Ubc7p-dependent, RING-H2-dependent self-ubiquitination when Hrd3p is absent (16). In a *hrd3Δ*-null mutant, the normal Hrd1p protein undergoes rapid, Ubc7p-dependent degradation with a half-life of 5–10 min, resulting in a drastic drop in Hrd1p steady-state level. In the same conditions, the C399S-RING mutant is completely stable. By removing Hrd3p, we could evaluate the stability of each chimeric Hrd1p protein, and thus the ability of each variant to engage Ubc7p *in vivo*. Strains with either native *HRD3* or a *hrd3Δ*-null allele expressing the 3HA-tagged Hrd1p chimeras were subjected to a cycloheximide chase assay. Hrd1p chimeras with RINGs from gp78, hsHrd1, or Praja1 were stable, while the native-RING Hrd1p protein underwent the expected, rapid self-degradation when Hrd3p was absent (Fig. 2*D*). Each chimeric Hrd1p was as stable as native-RING Hrd1p in the presence of Hrd3p (Fig. 2*D*), or Hrd1p with a C399S mutation that abrogates RING activity (data not shown). Thus, these heterologous RINGs did not engage Ubc7p *in vivo*, despite containing a similar RING-H2 motif.

Examination of the sequence alignment in Fig. 1 reveals an expansion in the Loop1 region of the Hrd1p RING motif not present in the other RINGs tested. We wondered if this unique sequence insertion in Hrd1p might determine the unique ability of Hrd1p to engage Ubc7p. To test this idea, we made a version of Hrd1p whose RING was missing the 13 proline-flanked residues (Hrd1p- Δ pro) in the Loop1 region as indicated in Fig. 1, and examined its stability in the presence and absence of Hrd3p. Surprisingly, Hrd1p- Δ pro was able to engage Ubc7p, as revealed by its Ubc7p-dependent degradation (Fig. 2*E*). However, this construct lost regulation by Hrd3p: in the presence or absence of Hrd3p, the Hrd1p- Δ pro construct was degraded at the same rate, although not as rapidly as Hrd1p with a normal RING. Hrd1p- Δ pro was stabilized by the removal of Ubc7p, or the addition of the inactivating C399S RING mutation (data not shown), indicating it engaged Ubc7p and underwent self-degradation. Also, overexpression of Hrd1p- Δ pro partially restored Hmg2p-GFP degradation (data not shown).

TDH3 promoter in strains with a *hrd1Δ* null allele and Hmg2p-GFP. For each strain, fluorescence of 20,000 cells was measured by flow cytometry, and the mean fluorescence was plotted as in *B*. *D*, replaced RINGs in Hrd1p do not engage E2. WT and replaced-RING versions of Hrd1p-3HA were expressed from the *HRD1* promoter in strains with either a *hrd1Δ*-null allele (*HRD3*) or *hrd1Δ* and *hrd3Δ*-null alleles (*hrd3Δ*). Cycloheximide-chase assays were performed for the indicated number of hours to elucidate the stability of each Hrd1p variant. In the absence of Hrd3p, HA-tagged Hrd1p undergoes degradation (*top panel*), but the replaced-RING Hrd1p proteins did not. *E*, Loop1 portion of Hrd1p is not required for E2 engagement. A portion of the Hrd1p RING in Loop1 not shared with other RINGs tested (see Fig. 1, *asterisk*), was removed and this Δ pro version of Hrd1p-3HA (Δ pro) and WT RING-Hrd1p-3HA (WT) were tested as in *D*, with the addition of a *hrd1Δ*, *hrd3Δ*, and *ubc7Δ*-null allele strain (*hrd3Δ*, *ubc7Δ*), revealing the Ubc7p dependence of Hrd1p and Hrd1p- Δ pro degradation.

Determinants of RING-E2 Fidelity for Hrd1p

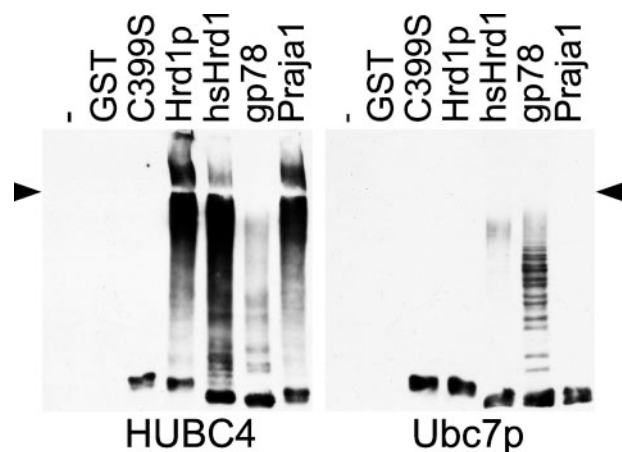


FIGURE 3. Lone RING motifs used to replace Hrd1p RING function *in vitro*. Ubiquitination reactions were run with GST fusions to each RING motif indicated, and either HUBC4 or Ubc7p as the E2. Immunoblotting of total reaction mix samples with anti-ubiquitin antibody revealed which RING motifs could form high molecular weight polyubiquitin chains. Arrowheads indicate the boundary between 8% running gel and 4% stacking gel.

Thus, the Loop1 sequence in Hrd1p is not the source of Ubc7p-specificity. This is consistent with structural analyses of E2-RING ligase complexes that suggest the Loop2 residues are involved in making E2 contacts, while Loop1 residues predominantly contact other residues in the E3 (20, 21).

Despite the apparent similarity of the RINGs, particularly in the Loop2 region, we next evaluated if the failure of the substituted RINGs to engage Ubc7p was caused by their intrinsic inability to recognize Ubc7p, by testing the biochemical activity of each isolated RING motif. Many RING-containing proteins will catalyze self-ubiquitination *in vitro* when combined with E1, E2, ubiquitin, and ATP (9, 10, 15, 23, 38). We adapted this approach to study the isolated RING motifs in otherwise identical fusions with GST, using both authentic Ubc7p or the widely used and highly promiscuous HUBC4. Recombinant Ubc7p was expressed from the pTYB2 vector as an intein-cleavable fusion to a chitin-binding domain (CBD/intein), and purified using chitin affinity beads (52). Addition of reducing-agent stimulates the intein protein-cleavage reaction, liberating free Ubc7p from the resin. *In vitro* reactions were run by combining ATP, ubiquitin, E1, E2, and affinity-purified GST-RING fusions. The formation of polyubiquitin chains in the reaction mixes was evaluated directly by SDS-PAGE and anti-ubiquitin immunoblotting. The isolated RINGs from Hrd1p, hsHrd1, gp78, or Praja1 all catalyzed polyubiquitin formation with the HUBC4 enzyme (Fig. 3, left panel) showing that the RING motifs possessed autonomous ubiquitin ligase activity. This activity required the presence of an active RING motif, as revealed by the inactivity of the GST alone and C399S RING controls. In the same assay using Ubc7p as E2, the mammalian gp78 RING showed significant ubiquitination activity with yeast Ubc7p, the hsHrd1 RING showed slight activity, and the Praja1 RING showed no ubiquitination, as did negative controls (Fig. 3, right panel). Surprisingly, the Hrd1p RING showed no formation of polyubiquitin with Ubc7p despite its natural role using Ubc7p *in vivo*. Thus, the gp78 RING could engage Ubc7p *in vitro*, but could not do so when part of full-length Hrd1p *in vivo*. Conversely, the Hrd1p RING could not engage Ubc7p *in vitro*, while it was the only RING tested that could function in full-length Hrd1p *in vivo*. Thus, lone RING motifs can indeed exhibit E3 activity as well as E2 selectivity. However, in these examples the specificity was entirely different from that of the full-length ligase functioning *in vivo*. We have used this “molecular irony” as a starting point to discern the conditions and requirements for biochemical study of Hrd1p. The correct *in vitro* conditions for accurate, biologically relevant E2 engagement by Hrd1p will not merely allow the Hrd1p RING to function with Ubc7p, but also prohibit the gp78 RING from engaging Ubc7p as observed *in vivo*.

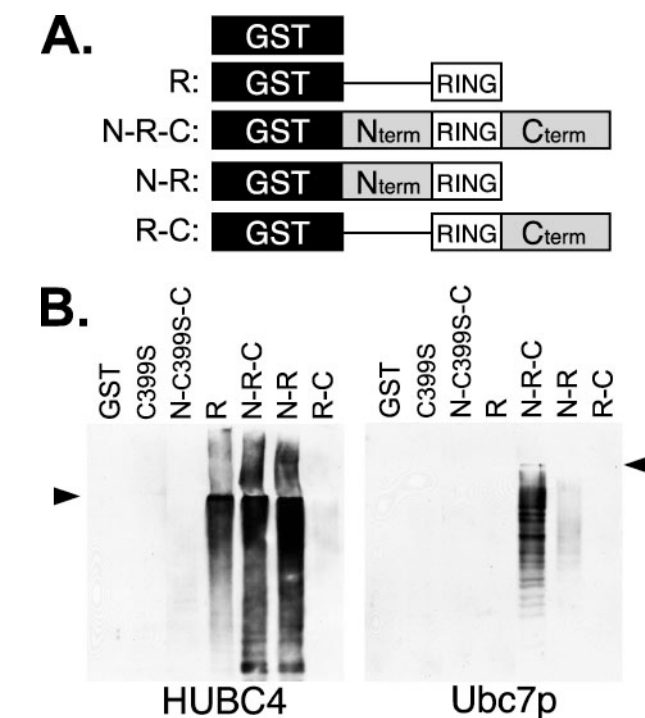


FIGURE 4. Effect of Hrd1p N or C RING-flanking regions on activity of GST-RING fusions. A, GST fusions to the RING of Hrd1p were made that also contained portions of cytoplasmic Hrd1p N-terminal and/or C-terminal to RING. N signifies 62 residues from the cytoplasmic domain N-terminal to RING. C signifies the 132 residues C-terminal to RING. B, GST fusions were tested in ubiquitination assays *in vitro* using HUBC4 or Ubc7p as the E2. Immunoblotting of total reaction mixes with anti-ubiquitin revealed which portions of Hrd1p could form high molecular weight polyubiquitin chains. Arrowheads indicate boundary between 8% running gel and 4% stacking gel.

The Hrd1p RING motif was necessary for Ubc7p engagement *in vivo*, but the lone Hrd1p RING could not use this E2 *in vitro*. We next asked if other portions of the Hrd1p cytoplasmic domain were required for RING-dependent engagement of Ubc7p. We produced Hrd1p-GST fusions with Hrd1p cytoplasmic domain regions flanking either or both sides of the RING motif (Fig. 4A). These included a construct in which the Hrd1p RING was flanked by 62 N-terminal residues and 132 C-terminal residues (GST-N-R-C), a construct with only the N-flanking portion and RING (GST-N-R), and a construct with only the C-flanking portion and RING (GST-R-C). *In vitro* ubiquitination reactions were run with equal concentrations of these GST fusions, using HUBC4 as positive control to confirm activity of the test proteins (Fig. 4B, right panel). GST-R, GST-N-R-C, and GST-N-R showed strong ubiquitination with HUBC4 (Fig. 4B, right panel). Although GST-R-C showed little

Determinants of RING-E2 Fidelity for Hrd1p

ubiquitination with HUBC4, it was active with HUBC4 when tested at higher concentrations (data not shown), as used previously (9). We then tested the fusions for function with Ubc7p. As expected, the lone Hrd1p RING (GST-R) was inactive, as was the GST-R-C extension, while GST-N-R had some capacity to employ Ubc7p. However, the presence of both flanks in GST-N-R-C allowed strong activity with Ubc7p (Fig. 4B, left panel), and this activity was entirely lost by mutation of the RING to the inactive form (GST-N-C399S-C). Thus, the presence of both the Hrd1p N and C flanks were needed for engagement of Ubc7p by the Hrd1p RING.

The lone gp78 RING recognized Ubc7p *in vitro*, but failed to function in the context of full length Hrd1p. We wondered if the longer sequences of Hrd1p that allow the natural RING to engage Ubc7p *in vitro* would also preclude use of this E2 by the gp78-RING. We made and tested the analogous, extended N- and C-fusions with the gp78 RING (GST-N-gp78-C). As shown in direct comparison, the GST-N-gp78-C fusion was much less active with Ubc7p than the GST-N-R-C with native Hrd1p RING (Fig. 5, top panel), while this fusion could still employ HUBC4 (data not shown). Thus, the sequences flanking the Hrd1p RING play a critical role both in allowing productive engagement of Ubc7p by the natural RING, and inhibiting this ability in the similar gp78 RING. Taken alone, these results would indicate that the RING-flanking sequences are sufficient to impose the stringent requirement for the native Hrd1p RING *in vivo*. However, the analyses below reveal critical roles for trans factors and membrane context in addition to these *in cis* determinants.

Ubc7p is presented to membrane-bound Hrd1p by the ER-localized anchoring protein Cue1p (36). This protein has a single N-terminal membrane span and a cytoplasmic C-terminal region that strongly binds Ubc7p, imparting surface ER localization to this otherwise soluble E2. The Cue1p protein is absolutely required for HRD-dependent ERAD (32). There are at least two ways that Cue1p can affect Hrd1p-dependent ubiquitination. Cue1p increases the effective concentration of Ubc7p accessible to Hrd1p by anchoring it to the ER membrane; in a *cue1* Δ -null strain, Ubc7p is soluble and not ER-bound. However, we wondered if Cue1p binding might also increase the activity of Ubc7p. To address this, we purified a soluble Cue1p-Ubc7p heterodimer to test in our *in vitro* ubiquitination assay. We co-expressed Cue1p lacking its transmembrane-spanning anchor (Δ tmCue1p), and the Ubc7p-CBD/intein-fusion from a single bacterial expression plasmid. Chitin affinity purification of Ubc7p from the bacterial lysates resulted in co-purification of Ubc7p and the bound Δ tmCue1p. Coomassie staining of the eluted intein-cleaved product indicated that the two proteins bound with 1:1 stoichiometry (data not shown). Ubc7p or Ubc7p+ Δ tmCue1p were then tested in the *in vitro* ubiquitination assays by SDS-PAGE and ubiquitin immunoblotting of reaction mixtures, using identical concentrations of Ubc7p in both reactions. In contrast to Ubc7p alone (Fig. 5, top panel), Δ tmCue1p-Ubc7p strongly enhanced the ubiquitination activity of GST-N-R and GST-N-R-C causing the appearance of very large polyubiquitin chains (Fig. 5, bottom panel). Strikingly, Δ tmCue1p-Ubc7p also allowed the GST-N-gp78-C construct to form polyubiquitin chains as

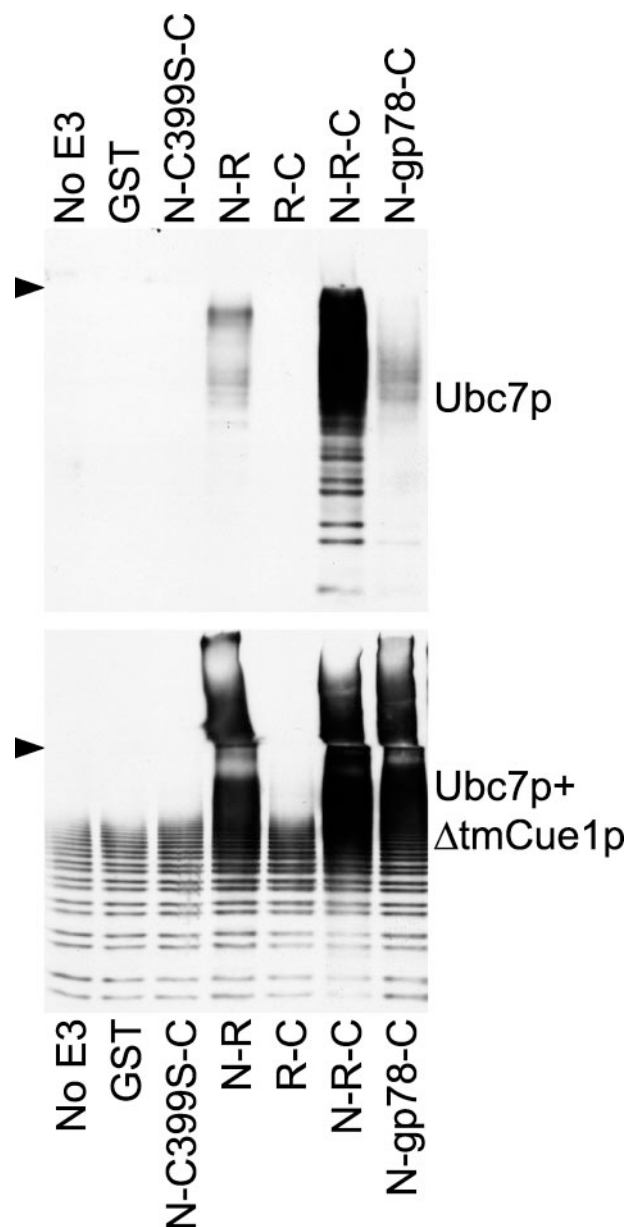


FIGURE 5. Cue1p affects the activity of Ubc7p. GST fusions were tested in ubiquitination assays *in vitro* using soluble Ubc7p (top panel), or soluble Δ tmCue1p-Ubc7p (bottom panel) as the E2 source. Assays were run as in Fig. 4, using the indicated GST fusion as the E3. Arrows indicate discontinuity between 8% running gel and 4% stacking gel.

effectively as the same protein with native Hrd1p RING (GST-N-R-C). Thus, the use of the Δ tmCue1p-Ubc7p heteromer completely removed the inhibitory effect of the N- and C-terminal flanks on the gp78 RING, making it as reactive as the analogous protein with the native Hrd1p RING.

Unlike free Ubc7p, Ubc7p with Δ tmCue1p was able to form intermediate size ubiquitin chains in the absence of any E3, as seen in the No E3, GST, and inactive RING controls. Immunoblotting of the E3-independent reactions suggested these products were polymers of ubiquitin and not the result of either Cue1p or Ubc7p multiubiquitination (data not shown). However, additional formation of large polyubiquitin chains caused by the presence of active RING proteins was easily distinguishable from this E3-independent activity.

Determinants of RING-E2 Fidelity for Hrd1p

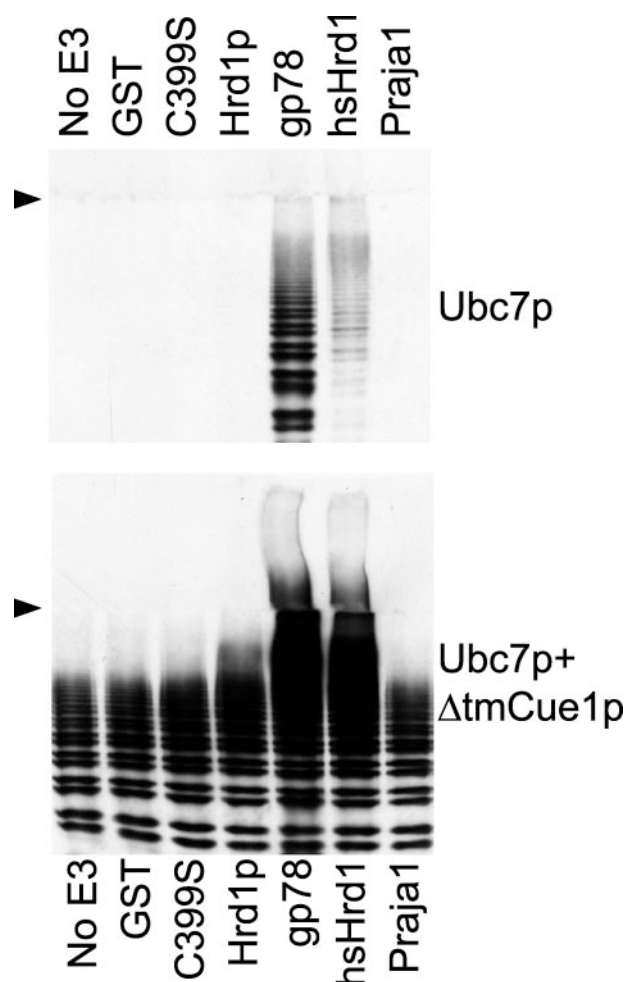


FIGURE 6. Cue1p enhances activity of Ubc7p without reducing specificity for lone RINGs. GST fusions used in Fig. 3 were tested with Ubc7p and Ubc7p + Δ tmCue1p. Cue1p substantially enhanced polyubiquitin chain formation only with RINGs that were also active with Ubc7p alone. Arrows indicate discontinuity between 8% running gel and 4% stacking gel.

Clearly, the presence of Δ tmCue1p increased both the basal and RING-stimulated formation of polyubiquitin chains by Ubc7p. Furthermore, this heteromer drastically increased the ability of the nearly inactive GST-N-R and GST-N-gp78-C proteins to form ubiquitin polymers. Thus, we wondered if the presence of the Cue1p binding partner somehow lessened the selectivity of Ubc7p for particular RINGs, making it more like HUBC4, or whether Cue1p simply increased the RING-specific activity of Ubc7p. To test this idea further, we evaluated the effect of Δ tmCue1p-Ubc7p on the ubiquitination activity of the isolated RING motifs fused to GST used earlier in Fig. 3. These experiments showed that Δ tmCue1p enhanced ubiquitination activity only in the presence of RINGs that could recognize free Ubc7p *in vitro* (Fig. 6). Only gp78-RING, and to a lesser extent hsHrd1-RING functioned with free Ubc7p, and only those RINGs produced very large ubiquitin chains with Δ tmCue1p-Ubc7p. The free Hrd1p-RING showed only very slight activity, and the Praja1-RING showed no reaction with either Ubc7p or Δ tmCue1p-Ubc7p. It is also noteworthy that, in Fig. 5, the RING constructs that were strongly activated by Δ tmCue1p were not completely inactive with Ubc7p alone. We conclude from these results that Cue1p did not participate in or modify

the selection of E3, but that it stimulated Ubc7p to be more active with those E3s it could engage.

Comparing the results using the authentic Hrd1p RING or the related gp78 RING raises an interesting dilemma. *In vivo*, the gp78 RING did not substitute for the Hrd1p RING when part of the full-length protein. This selectivity for the authentic RING was recapitulated *in vitro* with soluble proteins, using free Ubc7p and sufficient portions of the Hrd1p cytoplasmic domain: GST-N-R-C was reactive with Ubc7p, while GST-N-gp78-C was not. Taken alone, this result would indicate that high specificity for the authentic Hrd1p RING *in vivo* is imposed by the *in cis* context of the soluble cytoplasmic domain. That is, the Hrd1p RING functioned with Ubc7p in the large soluble N-R-C fusion, while the N-gp78-C fusion did not. However, when the Ubc7p was presented as part of the Cue1p-Ubc7p heterodimer, the N-gp78-C fusion functioned as well as the same construct with the native RING. *In vivo*, Cue1p is absolutely required for Hrd1p engagement of Ubc7p, but with inclusion of Cue1p, the RING specificity seen *in vivo* is no longer recapitulated in the soluble *in vitro* experiment. This implies that when Hrd1p is anchored in the ER membrane, other features impose the high selectivity for the Hrd1p RING and the observed intolerance *in vivo* for replacement with the RING from gp78, even when Cue1p is presenting Ubc7p. To explore this idea, we used a microsome assay we have recently developed for examination of full-length, ER-localized Hrd1p *in vitro* (42).

The various HA-tagged Hrd1p proteins studied in Fig. 2 were expressed from the strong *TDH3* promoter in *ubc7Δ*-null strains. Microsomes prepared from these strains provided membrane-localized, full-length Hrd1p with native or substituted RING. These microsomes were added to *in vitro* ubiquitination reactions with either HUBC4 or Ubc7p, and after incubation, the mix was solubilized in detergent buffer. Then full-length Hrd1p was immunoprecipitated and immunoblotted to evaluate Hrd1p self-ubiquitination.

The microsomal ubiquitination assay accurately reflected the *in vivo* engagement of Ubc7p by the Hrd1p variants. Wild-type Hrd1p showed abundant ubiquitination activity, the gp78-Hrd1p chimera was much less active and the hsHrd1p or Praja1 chimeras were nearly as low as the inactive-RING or *hrd1Δ*-null controls (Fig. 7, right panel). In microsome ubiquitination reactions with HUBC4, wild-type Hrd1p and the Hrd1p chimeras with hsHrd1 or Praja1 RING all showed substantial ubiquitination activity. However, the gp78-RING-Hrd1p was also inactive with this normally very promiscuous E2 (Fig. 7, left panels). Thus, when the gp78 RING chimera was evaluated in the context of ER-bound Hrd1p, it lacked activity for both Ubc7p and HUBC4. This result would not be predicted from the soluble *in vitro* studies above and indicated the importance of correct cell biological context in the study of these proteins.

The relative Ubc7p-dependent activities of full-length, membrane-localized, native Hrd1p and gp78-Hrd1p resembled the *in vitro* results observed with these soluble RINGs in Fig. 5 when Cue1p was absent. However, Cue1p was not absent from the microsomes. As expected for this integral membrane protein (36), nearly all of cellular Cue1p partitioned to the microsome fractions. Immunoblotting with anti-Cue1p antibodies (a

Determinants of RING-E2 Fidelity for Hrd1p

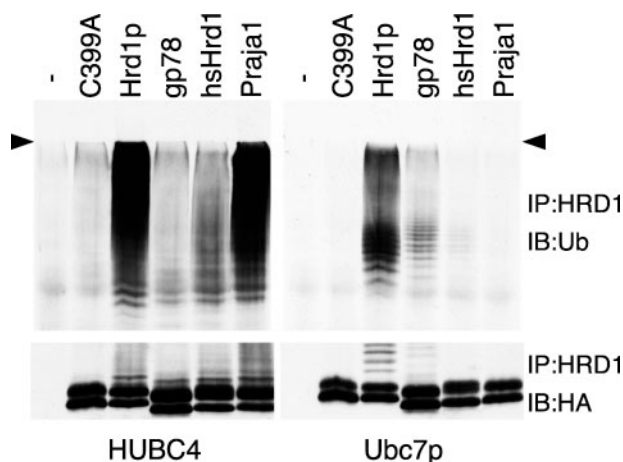


FIGURE 7. *In vitro* self-ubiquitination of RING-replaced Hrd1p in microsomes. Microsomes were prepared from strains expressing the indicated chimeric-RING-Hrd1p with 3HA epitope tag. *In vitro* ubiquitination reactions were prepared and run as described with either HUBC4 (left) or Ubc7p (right). Each Hrd1p was immunoprecipitated, and immunoblotted with either anti-ubiquitin antibody (upper panels) or anti-HA antibody (lower panels). Arrows indicate discontinuity between 8% running gel and 4% stacking gel.

gift from Thomas Sommer) confirmed that Cue1p in the microsome fractions was as abundant as Cue1p in whole cell lysates (data not shown). Thus, we wondered if Cue1p was required for Hrd1p-Ubc7p engagement in our microsome ubiquitination assay. We compared reactions using microsomes from strains with normal *CUE1* gene or a *cue1* Δ -null allele, using a range of Ubc7p concentrations. In contrast to the absolute *in vivo* requirement of Cue1p for Ubc7p-dependent activity, Cue1p moderately improved presentation of Ubc7p to Hrd1p in this microsome ubiquitination assay, shifting the concentration dependence by about 3-fold by visual inspection (Fig. 8, bottom, compare lanes 3–5 with lanes 7–9). This enhancement by Cue1p was specific for Ubc7p, as Cue1p showed no effect on the concentration curve for HUBC4-dependent ubiquitination of Hrd1p (Fig. 8, top). Although Cue1p showed Ubc7p-specific enhancement of Hrd1p microsome ubiquitination, the activity was not completely Cue1p-dependent as is observed *in vivo* (32).

To more closely approximate the *in vivo* conditions where strong Cue1p-dependence is manifest, we performed the assay using cytosolic extracts that provided endogenous Ubc7p for the assay. Cytosolic extracts were prepared from strains over-expressing epitope-tagged Ubc7p. Microsomes were prepared as before from strains with normal *CUE1* gene or a *cue1* Δ -null allele, incubated with the Ubc7p-containing cytosol, after which Hrd1p was immunoprecipitated and immunoblotted for ubiquitin. As was the case *in vivo*, *in vitro* Hrd1p ubiquitination was now strongly dependent on the presence of Cue1p in the microsomes (Fig. 9A, lanes 11 and 12). This Cue1p dependence was also observed by adding recombinant Ubc7p to cytosol prepared from *ubc7* Δ -null strains. By using identically tagged Ubc7p for the endogenous or recombinant Ubc7p, we determined the amount of E2 provided by the Ubc7p cytosol (Fig. 9B), and ran *in vitro* reactions using this range of added, recombinant Ubc7p. Again, we observed strong Cue1p dependence of Hrd1p ubiquitination (Fig. 9A, compare lanes 1–5 and 6–10). Curiously, the Ubc7p expressed in yeast cytosol appeared more

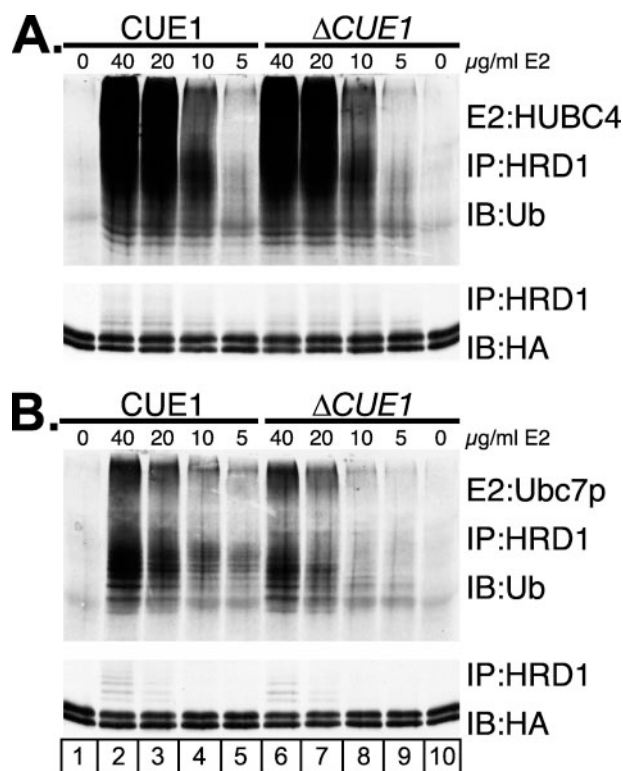


FIGURE 8. Participation of Cue1p in *in vitro* microsomal ubiquitination. A, Cue1p has no effect on the concentration of HUBC4 required for ubiquitination of Hrd1p. Microsomes were prepared from strains expressing Hrd1p-3HA. *In vitro* ubiquitination reactions were prepared with indicated serially diluted concentrations of HUBC4 (μ g/ml). Hrd1p was immunoprecipitated, and immunoblotted with either anti-ubiquitin antibody (upper panel) or anti-HA antibody (lower panel). B, Cue1p reduces the concentration of Ubc7p required for ubiquitination of Hrd1p. Same as in A, but with serially diluted Ubc7p.

active than the recombinant E2 (Fig. 9A, compare lane 11 with lanes 1–3), but in both cases Cue1p was absolutely required for Ubc7p-dependent polyubiquitination of membrane-bound Hrd1p.

The addition of cytosol to the *in vitro* reactions faithfully recapitulated the strong dependence on Cue1p for ubiquitination of Hrd1p. Thus, we tested if these conditions would allow the gp78-RING substituted Hrd1p to function, as was the case with the soluble chimeric protein. Despite the fact that the Ubc7p in this assay was presented by the Cue1p anchor, the gp78 chimera was still significantly less active than the native Hrd1p protein, (Fig. 10A). Importantly, the small amount of gp78 chimeric ubiquitination was fully Cue1p-dependent, confirming that the Ubc7p was presented to the chimera as part of the Cue1p-Ubc7p heteromer. Nevertheless, the activity of the gp78 chimera was much lower than the native protein, indicating again that the cell biological context imposed restrictions on the Hrd1p ligase not observed with the analogous soluble proteins.

The above biochemical studies used self-ubiquitination to examine the requirements for observing physiologically relevant Hrd1p action. With this approach, we have shown that the high specificity for the Hrd1p RING depended on *cis* flanking sequences and the presence of Hrd1p in the correct context of the ER membrane. Self-ubiquitination is a straightforward way

Determinants of RING-E2 Fidelity for Hrd1p

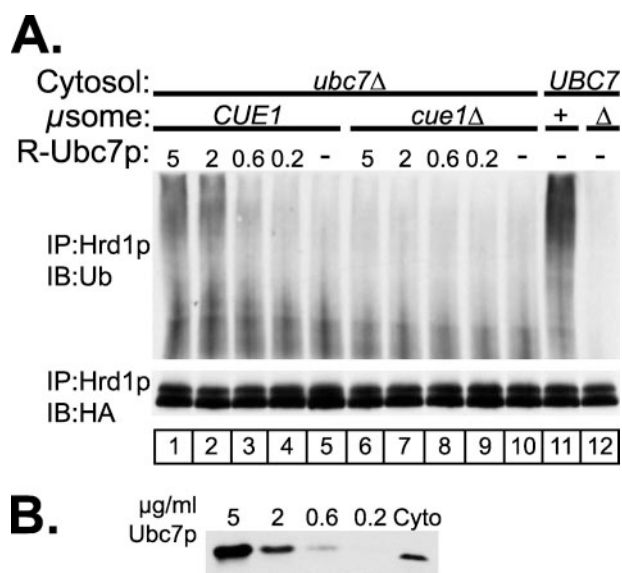


FIGURE 9. *In vitro* microsomal Hrd1p self-ubiquitination is strongly Cue1p-dependent in the presence of cytosol. A, ubiquitination of Hrd1p in cytosol is strongly Cue1p-dependent. Cytosol was prepared from strains with either a *ubc7Δ*-null allele (*ubc7Δ*) or from strains overexpressing Ubc7p-2HA (*UBC7*). Microsomes were prepared from strains expressing Hrd1p-3HA and with either native Cue1p (*CUE1*, +) or a *cue1Δ*-null allele (*cue1Δ*, Δ). Reactions with *ubc7Δ* cytosol were supplemented with the indicated concentrations (μg/ml) of recombinant Ubc7p-2HA (R-Ubc7p). The resultant ubiquitination reactions were immunoprecipitated with anti-Hrd1p antibodies and immunoblotted with either anti-ubiquitin antibody (upper panel) or anti-HA antibody (lower panel). B, determination of Ubc7p concentration in cytosolic extract. Cytosol prepared from strains overexpressing Ubc7p-2HA was compared with known concentrations of recombinant Ubc7p-2HA by immunoblotting with anti-HA antibody. Ubc7p-2HA at indicated concentrations (μg/ml) were loaded next to cytosolic extract (Cyto).

to study the action of ubiquitin ligases: however, their ultimate function is to catalyze ubiquitination of substrates, such as Hmg2p in the case of Hrd1p. Thus, we extended our *in vitro* analysis with a direct test of substrate ubiquitination (42), using Hmg2p, a natural substrate of Hrd1p-dependent ERAD (28). Hmg2p-GFP was expressed in the microsome strain along with Hrd1p, with a *ubc7Δ*-null allele to preclude ubiquitination until the E2 is introduced in the *in vitro* reaction. These microsomes were prepared as above and incubated in cytosol prepared from Ubc7p-expressing or *ubc7Δ*-null strains. Hmg2p-GFP ubiquitination was examined by immunoprecipitation with anti-GFP antibodies followed by immunoblotting for ubiquitin. Ubiquitin transfer to Hmg2p in this assay is entirely dependent on Hrd1p and Ubc7p (42). As expected, Hmg2p-GFP ubiquitination was entirely dependent on the presence of both Ubc7p and Cue1p (Fig. 10B). Moreover, ubiquitination of Hmg2p-GFP was proportional to the ubiquitination of Hrd1p in identical conditions (compare Figs. 10, A and B). Native-RING Hrd1p was able to support transfer of ubiquitin to Hmg2p-GFP as well as the previously observed self-ubiquitination. By contrast, gp78-RING Hrd1p showed little transfer of ubiquitin to Hmg2p-GFP, in accord with its weak self-ubiquitination. Ubiquitination of Hmg2p-GFP by native Hrd1p was ~9-fold more than that seen with the gp78-Hrd1p. This correlates well with the results seen by flow cytometry in Fig. 2C where at similar levels of ligase expression, the gp78-Hrd1p showed about 8-fold less effect on Hmg2p-GFP levels *in vivo* than authentic Hrd1p. The similarity

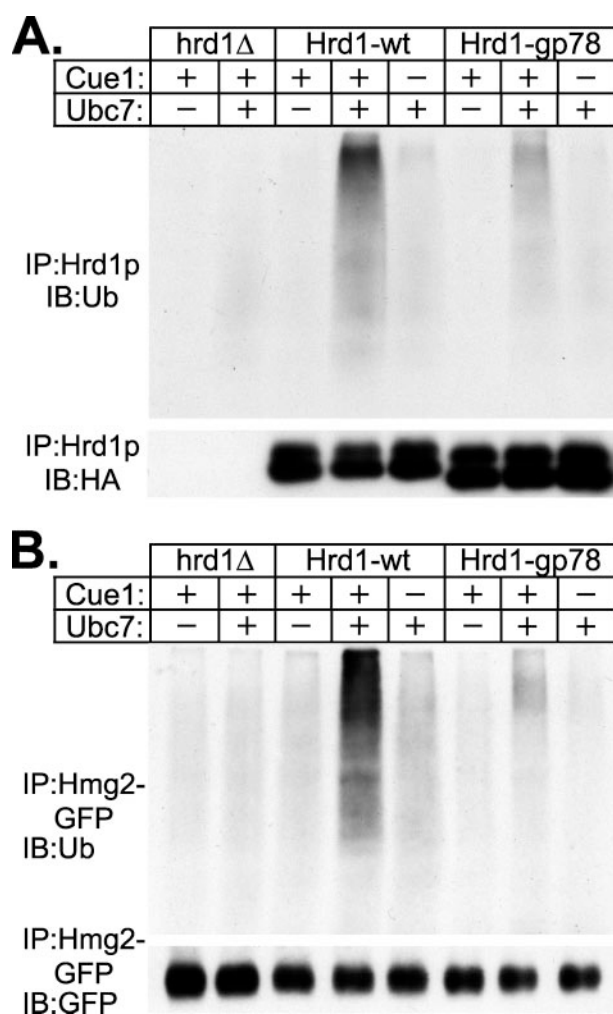


FIGURE 10. Comparison of *in vitro* Hrd1p self-ubiquitination and Hrd1p-catalyzed ubiquitination of Hmg2p-GFP. A, ubiquitination of Hrd1p with WT or gp78 RING is highly Cue1p-dependent. Microsomes were prepared from strains with either no Cue1p or native Cue1p and expressing no Hrd1p (*hrd1Δ*), epitope-tagged Hrd1p with WT RING (Hrd1-WT), or epitope-tagged Hrd1p with gp78-RING (Hrd1-gp78) as indicated. Cytosol was prepared from strains without Ubc7p, or overexpressing Ubc7p, as indicated. Ubiquitination reactions were immunoprecipitated with anti-Hrd1p antibody, and immunoblotted with either anti-ubiquitin antibody (upper panel) or anti-HA antibody (lower panel). B, ubiquitination of Hmg2p-GFP correlates with ubiquitination of the Hrd1p construct expressed. Hmg2p-GFP was expressed in the microsome strains used in 10A. A portion of the same reactions used in 10A were immunoprecipitated with anti-GFP antibody, and immunoblotted with either anti-ubiquitin antibody (upper panel) or anti-GFP antibody (lower panel).

of self-ubiquitination and transfer function validates the use of self-ubiquitination as a readout of authentic Hrd1p ubiquitin ligase activity.

DISCUSSION

In these studies we have systematically examined the requirements of the Hrd1p ubiquitin ligase for selective function with its preferred E2, Ubc7p. Our purpose was 2-fold: to better understand the conditions and requirements for study of Hrd1p *in vitro*, and to delineate conditions or principles that may be operating in other ligases.

The RING motif is necessary for engagement of E2s in many ubiquitin ligases, and makes contacts with the E2 molecule in the few structures that have been resolved (20–22). Thus, we

began by testing *in vivo* the importance of the native Hrd1p RING motif. Because RING removal or inactivation was already known to eliminate Hrd1p function, RING sequences from other ubiquitin ligases were used to precisely replace the native RING sequence (Fig. 1) in full-length native-level Hrd1p. The RING sequences were chosen from known ubiquitin ligase proteins, including homologs of Hrd1p. Despite this, the native RING motif was essential for functional engagement of Ubc7p by the Hrd1p protein; the gp78 RING provided very little activity in the Hrd1p protein, and hsHrd1 and Praja1 RINGs were completely non-functional in this context. This was somewhat surprising, because gp78 and hsHrd1 are the most closely related mammalian proteins to Hrd1p. Like Hrd1p, they participate in ERAD, and gp78 performs ERAD with Ube2g2, an E2 homologous to Ubc7p (17, 33). To test if the Hrd1p RING was sufficient to specify Ubc7p engagement, we studied the previously tested RING motifs in isolation by expressing recombinant GST-RING fusions, with either the widely-used E2 HUBC4, or authentic Ubc7p purified using an intein-fusion approach. Surprisingly, the gp78 RING engaged Ubc7p while the Hrd1p RING did not, although both could function with the promiscuous HUBC4. This inversion of the expected specificity revealed that conditions *in vivo* imparted constraints on E2-E3 pairing that the simplest direct assay of the soluble RING motifs did not.

An *in vitro* assay with the correct specificity as observed *in vivo* should permit Ubc7p to function with the Hrd1p RING, and restrict Ubc7p function with the gp78 RING. We used the gp78 and Hrd1p RING pair to evaluate the features and factors that bring about preference for the Hrd1p RING *in vivo*. The experiments revealed that a combination of conditions operate to this end. The *cis* sequence context of the cytoplasmic RING domain played a critical role, in that both the N- and C-terminal regions were required for robust use of Ubc7p by the Hrd1p RING. This was not simply due to the *cis* elements making the RING active, since the isolated Hrd1p RING was quite efficient at engaging another E2. Furthermore, these same flanking sequences made the gp78 RING less efficient at engaging Ubc7p, while retaining engagement of HUBC4. Taken alone, these data might be thought to completely explain the *in vivo* results, in which the authentic RING functions with Ubc7p but the gp78 RING does not. However, inclusion of Cue1p in our *in vitro* reactions showed that the actual case is more complex. When co-purified Δ tmCue1p-Ubc7p protein was used as the E2, the N-gp78-C fusion was equally active as the N-R-C fusion with the Hrd1p RING. This restoration of activity to the N-gp78-C fusion by the presence of Δ tmCue1p indicated that the N and C *cis* flanking regions were not the sole cause of gp78 RING inactivity in full-length Hrd1p *in vivo*. Moreover, inclusion of Cue1p is biologically relevant since Cue1p is absolutely required for Ubc7p function *in vivo* (32, 36).

In the context of the full-length, membrane-anchored protein, the gp78 RING was significantly less active with Ubc7p, and was similarly inactive with HUBC4. Even in the presence of cytosol, where the *in vitro* activity of Ubc7p was completely dependent on Cue1p, the gp78 RING-substituted Hrd1p was similarly less active than the native Hrd1p protein. This was distinct from the behavior of the large soluble Hrd1p fusion with gp78 RING, which reacted efficiently with Δ tmCue1p-

		Ubiquitination	
		Hrd1p RING	gp78 RING
GST-RING	- Cue1p	-	+
	+ Cue1p	-	+
GST-N-RING-C	- Cue1p	+	-
	+ Cue1p	+	+
Hrd1p in microsomes	- Cue1p	+	-
	+ Cue1p	+	-
Hrd1p in microsomes +cytosol	- Cue1p	-	-
	+ Cue1p	+	-
<i>in vivo</i>	- Cue1p	-	-
	+ Cue1p	+	-

FIGURE 11. Summary of *in vitro* function of Hrd1p and gp78 RINGs. Under the various conditions tested the Hrd1p and gp78 RINGs only recapitulated both the RING specificity and Cue1p dependence observed *in vivo* (bottom) when examined in the context of full-length microsomal Hrd1p in the presence of cytosol.

Ubc7p, and with HUBC4. Thus, the correct analysis of E2 selection by the Hrd1p-RING domain required being in the membrane-bound context, since that was the condition where the *in vivo* behavior of the native and chimeric Hrd1p proteins was recapitulated *in vitro*.

Many studies of E3 ligases, including our earlier work, are performed with partial, RING-containing portions of the E3 proteins, and/or convenient heterologous E2s (9, 10, 15, 33). In this systematic analysis of the requirements for highly specific RING and E2 function of Hrd1p *in vivo*, it is clear that a variety of conditions strongly determine these features of Hrd1p that were not included in our earlier assays. In fact, each alteration from lone RING to full-length membrane-bound Hrd1p caused a change in the use of RING and E2. The requirements for Ubc7p to both engage Hrd1p RING and exclude gp78 RING are more readily evaluated in table form (Fig. 11). This table summarizes Hrd1p RING or gp78 RING activity and Cue1p-dependence in each of the *in vitro* assays and *in vivo*. As can be seen, each new condition allowed a different result, and the only condition that faithfully recapitulated the *in vivo* RING and E2 selectivity was examination of the full-length protein in its membrane of origin. At present, we do not know if this restrictive behavior that results in E2 and RING selectivity is due to *cis* elements in the membrane anchor of Hrd1p, or to the proximity of the ER surface. An examination of the activity of full-length Hrd1p in micelles, or other circumstances that can separate these contributions may reveal the underpinning of this context effect. Additionally, the strong Cue1p dependence observed *in vivo* was seen *in vitro* only with full-length Hrd1p in microsomes incubated with cytosol. It may be that the lower

Determinants of RING-E2 Fidelity for Hrd1p

Ubc7p concentrations in cytosol amplified the need for the enhancing and concentrating effects of Cue1p. Alternatively, unknown factors in the cytosol may contribute to the need for Cue1p *in vivo*. In either case, it is noteworthy that the Ubc7p derived from cytosol was more potent than similar concentrations of recombinant Ubc7p. Collectively, these results justify the use of the microsome assay in studying Hrd1p, and show that caution must be applied when examining an E3 in conditions distinct from its native circumstances.

In these *in vitro* conditions we have examined the ubiquitination of Hrd1p itself to report on Hrd1p ubiquitin ligase function. Although Hrd1p is itself an ERAD substrate when out of stoichiometric balance with Hrd3p (16), we also wanted to observe Hrd1p transfer ubiquitin to a substrate other than itself. Indeed, full-length Hrd1p in microsomes with cytosol was able to transfer ubiquitin to Hmg2p-GFP. Like the Hrd1p ubiquitination assay, *in vitro* ubiquitin transfer to Hmg2-GFP observed *in vivo* RING selectivity. This activity was also Cue1p-dependent, validating the self-ubiquitination assay of Hrd1p function as a genuine readout of ubiquitin ligase activity. These results also suggest a quantitative correlation with *in vivo* degradation. *In vitro* Hmg2-GFP ubiquitination with native-RING-Hrd1p was eight to ten times better than with gp78-RING-Hrd1p. Interestingly, *in vivo* reduction of Hmg2p-GFP with overexpressed RING-Hrd1p (Fig. 2C) also showed an 8-fold greater effect by native-RING-Hrd1p than gp78-RING-Hrd1p, emphasizing that these more complex *in vitro* assay conditions correctly predict *in vivo* function.

In the studies above, we examined Hrd1p function alone, without its accessory protein Hrd3p, either because of isolation *in vitro* or because in the microsomal assay overexpressed Hrd1p is in excess of Hrd3p. When both Hrd1p and Hrd3p are present at normal levels, the Hrd1p protein is very stable and able to perform ERAD (16). It may be that one of the functions of Hrd3p is to bias the ligase activity away from Hrd1p self-ubiquitination and channel it toward substrate ubiquitination. Although we have not compared self-ubiquitination to substrate transfer when Hrd1p and Hrd3p are at normal levels, we are currently working on this more challenging assay. It is possible that other E3s have evolved regulatory factors like Hrd3p that could preferentially influence transfer of ubiquitin to either ligase or substrate, allowing regulation of E3 level through degradation.

The Hrd1p RING is distinguished from the other RINGs tested by an insert on the N-terminal-half (Loop1) of the RING motif (Fig. 1). The C-terminal-half (Loop2) of all the RINGs are quite similar. We surmised that the highly selective utilization of the Hrd1p RING *in vivo* would be due to this unique additional sequence in Loop1. We removed this sequence from Hrd1p and the resulting Hrd1p- Δ pro was still able to engage Ubc7p. Instead, Hrd1p regulation by Hrd3p was lost, suggesting involvement of a portion of the RING in the kind of self *versus* substrate regulation described above. The Loop1 expansion in Hrd1p is prevalent among the Hrd1p homologs in fungi, and is absent in the mammalian homologs. It is consistent that a portion of the Hrd1p RING which mediates regulation by Hrd3p resides in a region of the RING thought to be involved in E3-specific residue interactions, and not in interactions with E2s. Many RINGs have a large insertion in the Loop1 region,

including San1p and Hrt1/Roc1/Rbx1. It is as yet unclear how often these Loop1 regions are simply involved in maintaining the structure of the E3, or whether they facilitate an undiscovered means for regulation of those ligases. In addition to the structural predictions that Loop2 is involved in E2 interactions, domain swap experiments indicate that Loop2 in the Hrd1p RING is responsible for the ability to engage Ubc7p *in vivo* (data not shown). Thus the large insert in the Hrd1p RING was not the determining factor of Ubc7p engagement. Rather, subtle features of the RING domain determine the function of Hrd1p when present in the ER membrane.

Because Cue1p has been studied only in its ER-anchored state (32, 36, 53), it has not been clear whether Cue1p only plays a concentrating role by localizing Ubc7p to the ER surface, or if Cue1p additionally affects intrinsic Ubc7p activity. Our studies with soluble Δ mCue1p-Ubc7p complex clearly showed that this protein strongly affects the biochemistry of the E2, independent of any membrane-concentrating effects. Thus, Cue1p is an integral component of the Ubc7p E2. It will be interesting to see if the specificity or action of Ubc7p is altered by Cue1p. Despite its higher activity, the Δ mCue1p-Ubc7p still failed to react with Praja1 RING, and only poorly reacted with Hrd1p RING, implying that the E2 activity of Ubc7p was enhanced without changing specificity, but this must be examined in more detail. The effect of Cue1p allows the possibility that other E2 binding or interacting factors may similarly activate their cognate E2s.

gp78 and Hrd1p are related ubiquitin ligases with N-terminal transmembrane domains and soluble C-terminal RING-containing domains involved in ERAD, but there are several noteworthy differences. It is clear that Cue1p binds to Ubc7p (36), but how this Cue1p-Ubc7p complex is recruited to Hrd1p, if it is at all specifically recruited, is not understood. gp78 contains a CUE domain in its soluble cytoplasmic region, but it is not involved in recruiting the E2 Ube2g2 to gp78 (17). That is accomplished by a distinct Ube2g2-binding region, also in the soluble cytoplasmic region of gp78. Like other CUE proteins, the CUE domain of gp78 promotes binding to polyubiquitin, but yeast Cue1p is notable for its lack of polyubiquitin binding (54). Our work suggests that, like Ubc7p and Cue1p interaction in yeast, Ube2g2-binding by the cytosolic portion of gp78 in mammals may result in activation of Ube2g2.

Taken together, these studies indicate that the specific E3-E2 function of Hrd1p and Ubc7p is complex and involves multiple necessary conditions. These include the presence of *cis*-acting portions of the Hrd1p soluble cytoplasmic domain, the presence of the Ubc7p-activating Cue1p, and the placement of the Hrd1p ubiquitin ligase in the ER membrane, which all must be included in biochemical analyses to ensure that successful reconstitutions are physiologically meaningful ones as well.

Acknowledgments—We thank Allan M. Weissman for gp78 and Praja1 plasmids, Marjolein Kikkert and Emmanuel Wiertz for hsHrd1 plasmid, Thomas Sommer for Ubc7p plasmid and affinity-purified anti-Cue1p antibody, and Mark Wogulis and David K. Wilson for sharing their initial results purifying Ubc7p as an Intein-Chitin Binding Domain fusion. We also thank Robert Rickert and Michael David for FACScalibur flow cytometer access.

REFERENCES

- Petroski, M. D., and Deshaies, R. J. (2005) *Nat. Rev. Mol. Cell. Biol.* **6**, 9–20
- Nakayama, K. I., and Nakayama, K. (2006) *Nat. Rev. Cancer* **6**, 369–381
- Huang, T. T., and D'Andrea, A. D. (2006) *Nat. Rev. Mol. Cell. Biol.* **7**, 323–334
- Staub, O., and Rotin, D. (2006) *Physiol. Rev.* **86**, 669–707
- Hochstrasser, M. (1996) *Annu. Rev. Genet.* **30**, 405–439
- Hershko, A., and Ciechanover, A. (1998) *Annu. Rev. Biochem.* **67**, 425–479
- Pickart, C. M. (2001) *Annu. Rev. Biochem.* **70**, 503–533
- Seol, J. H., Feldman, R. M., Zachariae, W., Shevchenko, A., Correll, C. C., Lyapina, S., Chi, Y., Galova, M., Claypool, J., Sandmeyer, S., Nasmyth, K., and Deshaies, R. J. (1999) *Genes Dev.* **13**, 1614–1626
- Bays, N. W., Gardner, R. G., Seelig, L. P., Joazeiro, C. A., and Hampton, R. Y. (2001) *Nat. Cell Biol.* **3**, 24–29
- Swanson, R., Locher, M., and Hochstrasser, M. (2001) *Genes Dev.* **15**, 2660–2674
- Gardner, R. G., Nelson, Z. W., and Gottschling, D. E. (2005) *Cell* **120**, 803–815
- Fang, S., Lorick, K. L., Jensen, J. P., and Weissman, A. M. (2003) *Semin. Cancer Biol.* **13**, 5–14
- Hatakeyama, S., Yada, M., Matsumoto, M., Ishida, N., and Nakayama, K. I. (2001) *J. Biol. Chem.* **276**, 33111–33120
- Zhang, M., Windheim, M., Roe, S. M., Pegg, M., Cohen, P., Prodromou, C., and Pearl, L. H. (2005) *Mol. Cell* **20**, 525–538
- Lorick, K. L., Jensen, J. P., Fang, S., Ong, A. M., Hatakeyama, S., and Weissman, A. M. (1999) *Proc. Natl. Acad. Sci. U. S. A.* **96**, 11364–11369
- Gardner, R. G., Swarbrick, G. M., Bays, N. W., Cronin, S. R., Wilhovsky, S., Seelig, L., Kim, C., and Hampton, R. Y. (2000) *J. Cell Biol.* **151**, 69–82
- Chen, B., Mariano, J., Tsai, Y. C., Chan, A. H., Cohen, M., and Weissman, A. M. (2006) *Proc. Natl. Acad. Sci. U. S. A.* **103**, 341–346
- Weissman, A. M. (2001) *Nat. Rev. Mol. Cell. Biol.* **2**, 169–178
- Pickart, C. M., and Eddins, M. J. (2004) *Biochim. Biophys. Acta* **1695**, 55–72
- Zheng, N., Wang, P., Jeffrey, P. D., and Pavletich, N. P. (2000) *Cell* **102**, 533–539
- Zheng, N., Schulman, B. A., Song, L., Miller, J. J., Jeffrey, P. D., Wang, P., Chu, C., Koepf, D. M., Elledge, S. J., Pagano, M., Conaway, R. C., Conaway, J. W., Harper, J. W., and Pavletich, N. P. (2002) *Nature* **416**, 703–709
- Brzovic, P. S., Keefe, J. R., Nishikawa, H., Miyamoto, K., Fox, D., 3rd, Fukuda, M., Ohta, T., and Kleit, R. (2003) *Proc. Natl. Acad. Sci. U. S. A.* **100**, 5646–5651
- Katoh, S., Hong, C., Tsunoda, Y., Murata, K., Takai, R., Minami, E., Yamazaki, T., and Katoh, E. (2003) *J. Biol. Chem.* **278**, 15341–15348
- Brodsky, J. L., and McCracken, A. A. (1999) *Semin. Cell Dev. Biol.* **10**, 507–513
- Haynes, C. M., Caldwell, S., and Cooper, A. A. (2002) *J. Cell Biol.* **158**, 91–101
- Fang, S., Ferrone, M., Yang, C., Jensen, J. P., Tiwari, S., and Weissman, A. M. (2001) *Proc. Natl. Acad. Sci. U. S. A.* **98**, 14422–14427
- Amano, T., Yamasaki, S., Yagishita, N., Tsuchimochi, K., Shin, H., Kawahara, K., Aratani, S., Fujita, H., Zhang, L., Ikeda, R., Fujii, R., Miura, N., Komiya, S., Nishioka, K., Maruyama, I., Fukamizu, A., and Nakajima, T. (2003) *Genes Dev.* **17**, 2436–2449
- Hampton, R. Y., Gardner, R. G., and Rine, J. (1996) *Mol. Biol. Cell* **7**, 2029–2044
- Bordallo, J., Plemper, R. K., Finger, A., and Wolf, D. H. (1998) *Mol. Biol. Cell* **9**, 209–222
- Plemper, R. K., Egner, R., Kuchler, K., and Wolf, D. H. (1998) *J. Biol. Chem.* **273**, 32848–32856
- Wilhovsky, S., Gardner, R., and Hampton, R. (2000) *Mol. Biol. Cell* **11**, 1697–1708
- Gardner, R. G., Shearer, A. G., and Hampton, R. Y. (2001) *Mol. Cell. Biol.* **21**, 4276–4291
- Kikkert, M., Doolman, R., Dai, M., Avner, R., Hassink, G., van Voorden, S., Thanedar, S., Roitelman, J., Chau, V., and Wiertz, E. (2004) *J. Biol. Chem.* **279**, 3525–3534
- Ho, S. N., Hunt, H. D., Horton, R. M., Pullen, J. K., and Pease, L. R. (1989) *Gene (Amst.)* **77**, 51–59
- Horton, R. M., Hunt, H. D., Ho, S. N., Pullen, J. K., and Pease, L. R. (1989) *Gene (Amst.)* **77**, 61–68
- Biederer, T., Volkwein, C., and Sommer, T. (1997) *Science* **278**, 1806–1809
- Mori, S., Tanaka, K., Kanaki, H., Nakao, M., Anan, T., Yokote, K., Tamura, K., and Saito, Y. (1997) *Eur. J. Biochem.* **247**, 1190–1196
- Joazeiro, C. A., Wing, S. S., Huang, H., Levenson, J. D., Hunter, T., and Liu, Y. C. (1999) *Science* **286**, 309–312
- Hampton, R. Y., and Rine, J. (1994) *J. Cell Biol.* **125**, 299–312
- Guldener, U., Heck, S., Fielder, T., Beinbauer, J., and Hegemann, J. H. (1996) *Nucleic Acids Res.* **24**, 2519–2524
- Goldstein, A. L., and McCusker, J. H. (1999) *Yeast* **15**, 1541–1553
- Flury, I., Garza, R., Shearer, A., Rosen, J., Cronin, S., and Hampton, R. Y. (2005) *EMBO J.* **24**, 3917–3926
- Spang, A., and Schekman, R. (1998) *J. Cell Biol.* **143**, 589–599
- Zhong, X., Shen, Y., Ballar, P., Apostolou, A., Agami, R., and Fang, S. (2004) *J. Biol. Chem.* **279**, 45676–45684
- Song, B. L., Sever, N., and DeBose-Boyd, R. A. (2005) *Mol. Cell* **19**, 829–840
- Kaneko, M., Ishiguro, M., Niinuma, Y., Uesugi, M., and Nomura, Y. (2002) *FEBS Lett.* **532**, 147–152
- Allen, J. R., Nguyen, L. X., Sargent, K. E., Lipson, K. L., Hackett, A., and Urano, F. (2004) *Biochem. Biophys. Res. Commun.* **324**, 166–170
- Sasaki, A., Masuda, Y., Iwai, K., Ikeda, K., and Watanabe, K. (2002) *J. Biol. Chem.* **277**, 22541–22546
- Saha, T., Vardhini, D., Tang, Y., Katuri, V., Jogunoori, W., Volpe, E. A., Haines, D., Sidawy, A., Zhou, X., Gallicano, I., Schlegel, R., Mishra, B., and Mishra, L. (2006) *Oncogene* **25**, 693–705
- Cronin, S. R., Khoury, A., Ferry, D. K., and Hampton, R. Y. (2000) *J. Cell Biol.* **148**, 915–924
- Gardner, R., Cronin, S., Leader, B., Rine, J., and Hampton, R. (1998) *Mol. Biol. Cell* **9**, 2611–2626
- Chong, S., Mersha, F. B., Comb, D. G., Scott, M. E., Landry, D., Vence, L. M., Perler, F. B., Benner, J., Kucera, R. B., Hirvonen, C. A., Pelletier, J. J., Paulus, H., and Xu, M. Q. (1997) *Gene* **192**, 271–281
- Ravid, T., Kreft, S. G., and Hochstrasser, M. (2006) *EMBO J.* **25**, 533–543
- Shih, S. C., Prag, G., Francis, S. A., Sutanto, M. A., Hurley, J. H., and Hicke, L. (2003) *EMBO J.* **22**, 1273–1281

Supplemental Table 1. List of strains, and figures of usage.

Strain	Genotype	Figure
RHY2940	<i>MATα ade2-101 met2 lys2-801 his3Δ200 leu2Δ hmg1Δ::LYS2 hmg2Δ::HIS3 ura3-52::URA3::pTDH3-HMGcd::pTDH3-HMG2-GFP hrd1Δ::KanMX trp1::hisG::TRP1(pRH311)</i>	2A, 2B, 2D
RHY2941	<i>MATα ade2-101 met2 lys2-801 his3Δ200 leu2Δ hmg1Δ::LYS2 hmg2Δ::HIS3 ura3-52::URA3::pTDH3-HMGcd::pTDH3-HMG2-GFP hrd1Δ::KanMX trp1::hisG::TRP1::HRD1-3HA(pRH642)</i>	2A, 2B, 2D, 2E
RHY2943	<i>MATα ade2-101 met2 lys2-801 his3Δ200 leu2Δ hmg1Δ::LYS2 hmg2Δ::HIS3 ura3-52::URA3::pTDH3-HMGcd::pTDH3-HMG2-GFP hrd1Δ::KanMX trp1::hisG::TRP1::C399S-HRD1-3HA(pRH1245)</i>	2A, 2B, 2D
RHY2944	<i>MATα ade2-101 met2 lys2-801 his3Δ200 leu2Δ hmg1Δ::LYS2 hmg2Δ::HIS3 ura3-52::URA3::pTDH3-HMGcd::pTDH3-HMG2-GFP hrd1Δ::KanMX trp1::hisG::TRP1::PRAJ1-RING-HRD1-3HA(pRH1644)</i>	2A, 2B, 2D
RHY2946	<i>MATα ade2-101 met2 lys2-801 his3Δ200 leu2Δ hmg1Δ::LYS2 hmg2Δ::HIS3 ura3-52::URA3::pTDH3-HMGcd::pTDH3-HMG2-GFP hrd1Δ::KanMX trp1::hisG::TRP1::gp78-RING-HRD1-3HA(pRH1646)</i>	2A, 2B, 2D
RHY3508	<i>MATα ade2-101 met2 lys2-801 his3Δ200 leu2Δ hmg1Δ::LYS2 hmg2Δ::HIS3 ura3-52::URA3::pTDH3-HMGcd::pTDH3-HMG2-GFP hrd1Δ::KanMX trp1::hisG::TRP1::hsHrd1-RING-HRD1-3HA(pRH1883)</i>	2A, 2B, 2D
RHY2942	<i>MATα ade2-101 met2 lys2-801 his3Δ200 leu2Δ hmg1Δ::LYS2 hmg2Δ::HIS3 ura3-52::URA3::pTDH3-HMGcd::pTDH3-HMG2-GFP hrd1Δ::KanMX trp1::hisG::TRP1::pTDH3-HRD1-3HA(pRH730)</i>	2C
RHY2945	<i>MATα ade2-101 met2 lys2-801 his3Δ200 leu2Δ hmg1Δ::LYS2 hmg2Δ::HIS3 ura3-52::URA3::pTDH3-HMGcd::pTDH3-HMG2-GFP hrd1Δ::KanMX trp1::hisG::TRP1::pTDH3-PRAJ1-RING-HRD1-3HA(pRH1645)</i>	2C
RHY2947	<i>MATα ade2-101 met2 lys2-801 his3Δ200 leu2Δ hmg1Δ::LYS2 hmg2Δ::HIS3 ura3-52::URA3::pTDH3-HMGcd::pTDH3-HMG2-GFP hrd1Δ::KanMX trp1::hisG::TRP1::pTDH3-gp78-RING-HRD1-3HA(pRH1647)</i>	2C
RHY3710	<i>MATα ade2-101 met2 lys2-801 his3Δ200 leu2Δ hmg1Δ::LYS2 hmg2Δ::HIS3 ura3-52::URA3::pTDH3-HMGcd::pTDH3-HMG2-GFP hrd1Δ::KanMX trp1::hisG::TRP1::pTDH3-hsHrd1-RING-HRD1-3HA(pRH1912)</i>	2C
RHY2995	<i>MATα ade2-101 met2 lys2-801 his3Δ200 leu2Δ hmg1Δ::LYS2 hmg2Δ::HIS3 ura3-52::URA3::pTDH3-HMGcd::pTDH3-HMG2-GFP hrd1Δ::KanMX hrd3Δ::LEU2 trp1::hisG::TRP1::HRD1-3HA(pRH642)</i>	2D, 2E
RHY2998	<i>MATα ade2-101 met2 lys2-801 his3Δ200 leu2Δ hmg1Δ::LYS2 hmg2Δ::HIS3 ura3-52::URA3::pTDH3-HMGcd::pTDH3-HMG2-GFP hrd1Δ::KanMX hrd3Δ::LEU2 trp1::hisG::TRP1::PRAJ1-RING-HRD1-3HA(pRH1644)</i>	2D
RHY3001	<i>MATα ade2-101 met2 lys2-801 his3Δ200 leu2Δ hmg1Δ::LYS2 hmg2Δ::HIS3 ura3-52::URA3::pTDH3-HMGcd::pTDH3-HMG2-GFP hrd1Δ::KanMX hrd3Δ::LEU2 trp1::hisG::TRP1::gp78-RING-HRD1-3HA(pRH1646)</i>	2D
RHY3532	<i>MATα ade2-101 met2 lys2-801 his3Δ200 leu2Δ hmg1Δ::LYS2 hmg2Δ::HIS3 ura3-52::URA3::pTDH3-HMGcd::pTDH3-HMG2-GFP hrd1Δ::KanMX hrd3Δ::LEU2 trp1::hisG::TRP1::hsHrd1-RING-HRD1-3HA(pRH1883)</i>	2D

RHY3574	<i>MATα ade2-101 met2 lys2-801 his3Δ200 leu2Δ hmg1Δ::LYS2 hmg2Δ::HIS3 ura3-52::URA3::pTDH3-HMGcd::pTDH3-HMG2-GFP hrd1Δ::KanMX hrd3Δ::LEU2 ubc7Δ::NatR trp1::hisG::TRP1::HRD1-3HA(pRH642)</i>	2E
RHY4083	<i>MATα ade2-101 met2 lys2-801 his3Δ200 leu2Δ hmg1Δ::LYS2 hmg2Δ::HIS3 ura3-52::URA3::pTDH3-HMGcd::pTDH3-HMG2-GFP hrd1Δ::KanMX trp1::hisG::TRP1::Hrd1pΔpro-RING-HRD1-3HA(pRH1949)</i>	2E
RHY4090	<i>MATα ade2-101 met2 lys2-801 his3Δ200 leu2Δ hmg1Δ::LYS2 hmg2Δ::HIS3 ura3-52::URA3::pTDH3-HMGcd::pTDH3-HMG2-GFP hrd1Δ::KanMX hrd3Δ::LEU2 trp1::hisG::TRP1::hsHrd1-RING-HRD1-3HA(pRH1949)</i>	2E
RHY4097	<i>MATα ade2-101 met2 lys2-801 his3Δ200 leu2Δ hmg1Δ::LYS2 hmg2Δ::HIS3 ura3-52::URA3::pTDH3-HMGcd::pTDH3-HMG2-GFP hrd1Δ::KanMX hrd3Δ::LEU2 ubc7Δ::NatR trp1::hisG::TRP1::hsHrd1-RING-HRD1-3HA(pRH1949)</i>	2E
RHY3751	<i>MATα ade2-101 met2 lys2-801 his3Δ200 leu2Δ hmg2Δ::1MYC-HMG2 ura3-52::URA3::pTDH3-HMG2-GFP pep4Δ::HIS3 hrd1Δ::KanMX ubc7Δ::LEU2 trp1::hisG::TRP1::empty vector(pRH311)</i>	7, 10
RHY3752	<i>MATα ade2-101 met2 lys2-801 his3Δ200 leu2Δ hmg2Δ::1MYC-HMG2 ura3-52::URA3::pTDH3-HMG2-GFP pep4Δ::HIS3 hrd1Δ::KanMX ubc7Δ::LEU2 trp1::hisG::TRP1::pTDH3-HRD1-3HA(pRH730)</i>	7, 8, 9A, 10
RHY3753	<i>MATα ade2-101 met2 lys2-801 his3Δ200 leu2Δ hmg2Δ::1MYC-HMG2 ura3-52::URA3::pTDH3-HMG2-GFP pep4Δ::HIS3 hrd1Δ::KanMX ubc7Δ::LEU2 trp1::hisG::TRP1::pTDH3-PRAJ1-RING-HRD1-3HA(pRH1645)</i>	7
RHY3754	<i>MATα ade2-101 met2 lys2-801 his3Δ200 leu2Δ hmg2Δ::1MYC-HMG2 ura3-52::URA3::pTDH3-HMG2-GFP pep4Δ::HIS3 hrd1Δ::KanMX ubc7Δ::LEU2 trp1::hisG::TRP1::pTDH3-gp78-RING-HRD1-3HA(pRH1647)</i>	7
RHY3762	<i>MATα ade2-101 met2 lys2-801 his3Δ200 leu2Δ hmg2Δ::1MYC-HMG2 ura3-52::URA3::pTDH3-HMG2-GFP pep4Δ::HIS3 hrd1Δ::KanMX ubc7Δ::LEU2 trp1::hisG::TRP1::pTDH3-hsHrd1-RING-HRD1-3HA(pRH1912)</i>	7
RHY3764	<i>MATα ade2-101 met2 lys2-801 his3Δ200 leu2Δ hmg2Δ::1MYC-HMG2 ura3-52::URA3::pTDH3-HMG2-GFP pep4Δ::HIS3 hrd1Δ::KanMX ubc7Δ::LEU2 trp1::hisG::TRP1::pTDH3-C399A-HRD1-3HA(pRH1900)</i>	7
RHY3929	<i>MATα ade2-101 met2 lys2-801 his3Δ200 leu2Δ hmg2Δ::1MYC-HMG2 ura3-52::URA3::pTDH3-HMG2-GFP pep4Δ::HIS3 hrd1Δ::KanMX ubc7Δ::LEU2 cue1Δ::NatR trp1::hisG::TRP1::pTDH3-HRD1-3HA(pRH730)</i>	8, 9A, 10
RHY3930	<i>MATα ade2-101 met2 lys2-801 his3Δ200 leu2Δ hmg2Δ::1MYC-HMG2 ura3-52::URA3::pTDH3-HMG2-GFP pep4Δ::HIS3 hrd1Δ::KanMX ubc7Δ::LEU2 cue1Δ::NatR trp1::hisG::TRP1::pTDH3-gp78-RING-HRD1-3HA(pRH1647)</i>	10
RHY4295	<i>MATα ade2-101 met2 lys2-801 his3Δ200 leu2Δ hmg2Δ::1MYC-HMG2 ura3-52 pep4Δ::HIS3 hrd1Δ::KanMX ubc7Δ::LEU2 trp1::hisG::TRP1::pTDH3-Ubc7p-2HA(pRH373)</i>	9, 10
RHY4288	<i>MATα ade2-101 met2 lys2-801 his3Δ200 leu2Δ hmg2Δ::1MYC-HMG2 ura3-52 pep4Δ::HIS3 hrd1Δ::KanMX ubc7Δ::LEU2 trp1::hisG</i>	9, 10

Supplemental Table 2. List of plasmids used.

Plasmid	Construction
pRH311	pRS404, <i>TRP1</i> /YIp Genetics 122: 19-27 (May, 1989)
pRH642	<i>P_{HRD1}</i> -Hrd1p-3HA. <i>TRP1</i> /YIp Native promoter Hrd1p from <i>hrd1-1</i> complementing plasmid was subcloned into pRS404 to make pRH507. PCR SOEing was used to add the 3HA tag.
pRH1245	<i>P_{HRD1}</i> -C399S-Hrd1p-3HA. <i>TRP1</i> /YIp Gardner, R.G. et al. (2000) JCB 151(1)69-82
pRH1644	<i>P_{HRD1}</i> -Praja1-RING-Hrd1p-3HA. <i>TRP1</i> /YIp The Praja1 RING was amplified by PCR from p2641 (Lorick, K. L. et al. 1999) and PCR SOEing was used to join it to the <i>HRD1</i> sequences adjacent to the Hrd1p RING. This was then subcloned into pRH642 to make pRH1644.
pRH1646	<i>P_{HRD1}</i> -gp78-RING-Hrd1p-3HA. <i>TRP1</i> /YIp The gp78 RING was amplified by PCR from GST-gp78C2 (Fang weissman AM 2001) and PCR SOEing was used to join it to the <i>HRD1</i> sequences adjacent to the Hrd1p RING. This was then subcloned into pRH642 to make pRH1646.
pRH1883	<i>P_{HRD1}</i> -hsHrd1-RING-Hrd1p-3HA. <i>TRP1</i> /YIp The Hrd1p RING was amplified by PCR from a human Hrd1-containing plasmid (Marjolein Kikkert / Wiertz Lab) and PCR SOEing was used to join it to the <i>HRD1</i> sequences adjacent to the Hrd1p RING. This was then subcloned into pRH642 to make pRH1883.
pRH1949	<i>P_{HRD1}</i> - Δ proRING-Hrd1p-3HA. <i>TRP1</i> /YIp PCR SOEing was used to make a Hrd1p RING without the sequence encoding the Δ pro residues in the Loop1 region of the Hrd1p RING. This was then subcloned into pRH642 to make pRH1949.
pRH730	<i>P_{TDH3}</i> -Hrd1p-3HA. <i>TRP1</i> /YIp Gardner, R.G. et al. (2000) JCB 151(1)69-82
pRH1645	<i>P_{TDH3}</i> -Praja1-RING-Hrd1p-3HA. <i>TRP1</i> /YIp The Praja1 RING was amplified by PCR from p2641 (Lorick, K. L. et al. 1999) and PCR SOEing was used to join it to the <i>HRD1</i> sequences adjacent to the Hrd1p RING. This was then subcloned into pRH730 to make pRH1645.
pRH1647	<i>P_{TDH3}</i> -gp78-RING-Hrd1p-3HA. <i>TRP1</i> /YIp The gp78 RING was amplified by PCR from GST-gp78C2 (Fang weissman AM 2001) and PCR SOEing was used to join it to the <i>HRD1</i> sequences adjacent to the Hrd1p RING. This was then subcloned into pRH730 to make pRH1647.
pRH1912	<i>P_{TDH3}</i> -hsHrd1-RING-Hrd1p-3HA. <i>TRP1</i> /YIp A human Hrd1 RING-containing BglIII/NcoI fragment from pRH1883 was subcloned into pRH730.
pRH1900	<i>P_{TDH3}</i> -C399S-Hrd1p-3HA. <i>TRP1</i> /YIp PCR SOEing was used to generate the C399S point mutation, and this fragment was subcloned into pRH730 with BglIII/NsiI.
pRH1749	GST-Hrd1p-RING The Hrd1p RING was amplified by PCR from pRH642 and subcloned into pET42b(+) with NcoI and EcoRI.
pRH1750	GST-C399S-Hrd1p-RING The C399S-Hrd1p RING was amplified by PCR from pRH1245 and

	subcloned into pET42b(+) with NcoI and EcoRI.
pRH1751	GST-Praja1-RING The Praja1 RING was amplified by PCR from pRH1644 and subcloned into pET42b(+) with NcoI and EcoRI.
pRH1752	GST-gp78-RING The gp78 RING was amplified by PCR from pRH1646 and subcloned into pET42b(+) with NcoI and EcoRI.
pRH1915	GST-hsHrd1-RING The hsHrd1 RING was amplified by PCR from pRH1883 and subcloned into pET42b(+) with NcoI and EcoRI.
pRH1466	GST-R-C, GST fused to the C-terminal 203 amino acids of Hrd1p in pET42b(+) Bays, NCB
pRH1726	GST-N-R-C, GST fused to amino acids 262 to 551 of Hrd1p. Hrd1p sequence cut from pRH730 with BsrFI and SpeI, was subcloned into pRH1466 using AgeI and AvrII.
pRH1728	GST-N-gp78-C, GST fused to amino acids 262 to 551 of Hrd1p with gp78-replacement in RING. gp78-RING-Hrd1p sequence was cut from pRH1647 with BsrFI and SpeI, was subcloned into pRH1466 using AgeI and AvrII.
pRH1729	GST-N-R, GST fused to amino acids 262 to 419 of Hrd1p. Hrd1p sequence from a c-terminal truncation was cut from pRH1654 with BsrFI and SpeI, and subcloned into pRH1466 using AgeI and AvrII.
pRH1946	Ubc7p-Intein/Chitin Binding Domain. Ubc7p was amplified by PCR from pRH373(Gardner et al (2001) MCB) and subcloned into NEB IMPACT vector TYB2.
pRH1289	6HIS-E1 (mouse UBA1) Mori, S. et al. <i>European Journal of Biochemistry</i> 247 , 1190-6 (1997).
pRH1290	6HIS-HUBC4 Mori, S. et al. <i>European Journal of Biochemistry</i> 247 , 1190-6 (1997).
pRH2061	Δ TM Cue1p and Ubc7p-Intein/Chitin Binding Domain. Cue1p was amplified by PCR and subcloned into a pET vector with NdeI and XhoI to place Δ TM Cue1p sequence near a ribosomal binding site. Then, the pET vector's ribosomal binding site and, Δ TM Cue1p were amplified by PCR and subcloned into pRH1946 using PstI, and screened for correct orientation.
pRH1947	Ubc7p-2HA-Intein/Chitin Binding Domain. Ubc7p was amplified by PCR from pRH373(Gardner et al (2001) MCB) and subcloned into NEB IMPACT vector TYB2.
pRH1600	pRH730 was digested with AflIII followed by partial digestion with NcoI and reclosure. promoterless Hrd1p-3HA. <i>TRP1/YIp</i> .